



Calhoun: The NPS Institutional Archive
DSpace Repository

Theses and Dissertations

1. Thesis and Dissertation Collection, all items

1978-12

Investigation of pipe flow instability and results for wave number zero

Arnold, Michael James

<http://hdl.handle.net/10945/18472>

Downloaded from NPS Archive: Calhoun



<http://www.nps.edu/library>

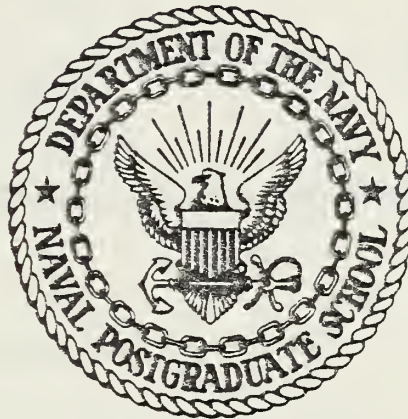
Calhoun is the Naval Postgraduate School's public access digital repository for research materials and institutional publications created by the NPS community. Calhoun is named for Professor of Mathematics Guy K. Calhoun, NPS's first appointed -- and published -- scholarly author.

Dudley Knox Library / Naval Postgraduate School
411 Dyer Road / 1 University Circle
Monterey, California USA 93943

DUDLEY KNOX LIBRARY
NAVAL POSTGRADUATE SCHOOL
MONTEREY, CA 93940

NAVAL POSTGRADUATE SCHOOL

Monterey, California



THESIS

INVESTIGATION OF PIPE FLOW INSTABILITY
AND RESULTS FOR WAVE NUMBER ZERO

by

Michael James Arnold

December 1978

Thesis Advisor:

T. H. Gawain

Approved for public release; distribution unlimited.

T187434

REPORT DOCUMENTATION PAGE		READ INSTRUCTIONS BEFORE COMPLETING FORM
1. REPORT NUMBER	2. GOVT ACCESSION NO.	3. RECIPIENT'S CATALOG NUMBER
4. TITLE (and Subtitle) Investigation of Pipe Flow Instability and Results for Wave Number Zero		5. TYPE OF REPORT & PERIOD COVERED Master's Thesis; December 1978
		6. PERFORMING ORG. REPORT NUMBER
7. AUTHOR(s) Michael James Arnold		8. CONTRACT OR GRANT NUMBER(s)
9. PERFORMING ORGANIZATION NAME AND ADDRESS Naval Postgraduate School Monterey, California 93940		10. PROGRAM ELEMENT, PROJECT, TASK AREA & WORK UNIT NUMBERS
11. CONTROLLING OFFICE NAME AND ADDRESS Naval Postgraduate School Monterey, California 93940		12. REPORT DATE December 1978
		13. NUMBER OF PAGES 122
14. MONITORING AGENCY NAME & ADDRESS (if different from Controlling Office)		15. SECURITY CLASS. (of this report) Unclassified
		15a. DECLASSIFICATION/DOWNGRADING SCHEDULE
16. DISTRIBUTION STATEMENT (of this Report) Approved for public release; distribution unlimited.		
17. DISTRIBUTION STATEMENT (of the abstract entered in Block 20, if different from Report)		
18. SUPPLEMENTARY NOTES		
19. KEY WORDS (Continue on reverse side if necessary and identify by block number) Pipe Flow Instability		
20. ABSTRACT (Continue on reverse side if necessary and identify by block number) Past research by Harrison and Johnston on the stability of pipe flow yielded only tenuous results owing to errors in setup of the problem and in formulation of the complex axis boundary conditions. Recent advances in the formulation of these boundary conditions and application of generalized stability criteria allowed an accurate numerical solution to be made for angular wave number zero. The results show that flow for this case is characterized by certain		

ABSTRACT (Cont'd)

instabilities that have not been previously identified in linearized studies of this type.

A nonuniform computational mesh was developed which provided dramatic reductions in computational time on a limited basis.

Two data reduction programs were also developed to process and display data generated by the main program.

Investigation of Pipe Flow Instability
and Results for Wave Number Zero

by

Michael James Arnold
Lieutenant, United States Navy
B.S., University of Idaho, 1969

Submitted in partial fulfillment of the
requirements for the degree of

MASTER OF SCIENCE IN AERONAUTICAL ENGINEERING

from the

NAVAL POSTGRADUATE SCHOOL
December 1978

ABSTRACT

Past research by Harrison and Johnston on the stability of pipe flow yielded only tenuous results owing to errors in setup of the problem and in formulation of the complex axis boundary conditions.

Recent advances in the formulation of these boundary conditions and application of generalized stability criteria allowed an accurate numerical solution to be made for angular wave number zero. The results show that flow for this case is characterized by certain instabilities that have not been previously identified in linearized studies of this type.

A nonuniform computational mesh was developed which provided dramatic reductions in computational time on a limited basis.

Two data reduction programs were also developed to process and display data generated by the main program.

TABLE OF CONTENTS

I.	INTRODUCTION -----	9
II.	THE VORTICITY TRANSPORT EQUATION -----	12
III.	NUMERICAL METHODS -----	17
IV.	RESULTS -----	25
	A. STABILITY -----	25
	B. PERTURBATION VELOCITY PLOTS -----	27
	C. STABILITY CONTOUR PLOTS -----	28
	D. NONUNIFORM MESH EFFECTS -----	29
	E. NUMERICAL ACCURACY -----	31
V.	CONCLUSIONS AND RECOMMENDATIONS -----	46
APPENDIX A:	DERIVATION OF VORTICITY TRANSPORT EQUATION COEFFICIENTS -----	48
APPENDIX B:	FINITE DIFFERENCE EQUATIONS -----	51
APPENDIX C:	NON-UNIFORM MESH -----	57
APPENDIX D:	DERIVATION OF PERTURBATION VELOCITIES -	65
COMPUTER PROGRAMS	-----	69
LIST OF REFERENCES	-----	121
INITIAL DISTRIBUTION LIST	-----	122

LIST OF FIGURES

3-1	Finite Difference Mesh -----	18
3-2	Basic Composition of Coefficient Arrays and Vector of Unknowns -----	20
4-1	Normalized Perturbation Velocity -----	34
4-2	Normalized Perturbation Velocity -----	35
4-3	Normalized Perturbation Velocity -----	36
4-4	Normalized Perturbation Velocity -----	37
4-5	Normalized Perturbation Velocity -----	38
4-6	Stability Contour Plot -----	39
4-7	Stability Contour Plot -----	40
4-8	γ^* Versus Number of Mesh Points, N -----	41
4-9	γ^* Versus Number of Mesh Points, N -----	42
4-10	γ^* Versus Mesh Parameter, Lambda -----	43
4-11	Normalized Perturbation Velocity -----	44
4-12	Normalized Perturbation Velocity -----	45
C-1	R versus η for Four Selected Values of Lambda-Axis Offset -----	63
C-2	R versus η for Four Selected Values of Lambda-Wall Offset -----	64

TABLE OF SYMBOLS

C	Constant in non-uniform mesh functions given by equations (C-32) and (C-40)
D, D^2, \dots	Partial derivatives with respect to r .
D^*, D^{*2}, \dots	Partial derivatives with respect to η .
e	Base of natural logarithms.
$\bar{e}_x, \bar{e}_r, \bar{e}_\theta$	Unit vectors along the x , r and θ axes in cylindrical coordinates.
F, G, H	Components of the velocity vector potential defined in equation (2-6).
f_{11}, f_{22}, \dots	Coefficients of D^*Q , $D^{*2}Q$, ... in equations (C-9) through (C-12) as defined in equations (C-13) through (C-22).
i	$+\sqrt{-1}$, the imaginary unit. Also used as an index in Section III and Appendix D.
N	The number of interior points in the finite difference mesh of Section III.
O	Symbol denoting the phrase "of order".
Q	The component of the velocity vector potential derived from the component H by the change of variable, $H = rQ$.
R_e	Reynolds number based on mean velocity and pipe radius.
t	Time.
U	The streamwise velocity in Pipe Poiseuille Flow as defined by equation (2-11).
u, v, w	Components of the complex perturbation velocity defined in equation (D-1).
\bar{W}	Complex vector potential of perturbation velocity defined in equation (D-2).
x, r, θ	Cylindrical coordinates.
α	$\alpha_R + i\alpha_I$. Complex wave number of the perturbation in the x -direction.

β	in. Complex wave number of the perturbation in the θ direction, where $n = 0, 1, 2, 3, \dots$
δ	$1/(N+1)$. The r or η increment in the finite difference approximations of the derivatives of Q .
η	The independent variable replacing r in the nonuniform mesh of Appendix C.
γ	$\gamma_R + i\gamma_I$. Complex frequency of the perturbation.
$\bar{\Gamma}$	The vorticity transport equation expressed in abbreviated notation as defined in equation (2-7).
$\Gamma_x, \Gamma_r, \Gamma_\theta$	The components of $\bar{\Gamma}$ in cylindrical coordinates as defined in equation (2-7).
λ	Mesh offset parameter as defined in equations (C-32) and (C-40).
∇	Linear vector operator (nabla)
\times	Vector cross-product operator.
[]	Brackets enclosing a matrix.
{ }	Brackets enclosing a column vector.

I. INTRODUCTION

The problem of finding an analytical solution to the pipe flow stability problem has been pursued actively ever since the classical experiments of Osborne Reynolds [10] about 100 years ago. Up to now, however, no investigation has been able to satisfactorily predict flow instabilities, although many approaches have been taken.

Salwen and Grosch [11] studied pipe flow with various angular wave numbers and sinusoidal streamwise perturbations and concluded that it was stable for all axial and angular wave numbers. Perturbations with exponential growth in space but a purely sinusoidal time variation were researched by Garg and Rouleau [2] and those with both exponential growth in space and in time by Gill [3]. Both concluded that the flows were stable.

Because of this inability of linear theory to account for experimental fact, explanations by Davey and Drazin [1] involving finite disturbances and by Huang and Chen [5] and Leite [7] involving conditions at the pipe entrance have been offered. While these investigations have indeed shown instabilities to exist, a completely general solution to the linear problem has never been achieved.

Recently a more general theory was presented by Harrison [4] and further investigated by Johnston [6]. These two studies, however, failed to produce conclusive results due

to mathematical errors in the problem setup and inadequate formulation of the boundary conditions at the axis. Gawain [9] has subsequently formulated the axis boundary conditions in a new way which corrects the previous discrepancies and promises further advances.

For angular wave number, n , equal to zero, radical simplifications result in the governing equations (Section II), indicating that this case should be approached first. This investigation centers on that case.

Preliminary checks using the computer program of Ref. 6 revealed that, of the two eigenfunctions, G and H , which occur in this problem and which are uncoupled for $n = 0$, the latter appeared to be the more critical. Hence the present research was arbitrarily restricted to investigation of the stability of eigenfunction H . A similar study of the other eigenfunction, G , for $n = 0$ remains to be completed at some future time. Comparable calculations for other wave numbers ($n = 1, 2, 3, \dots$) also remain to be accomplished in the future. Extensive and systematic calculations of this type will be essential to provide the factual basis for a comprehensive theory of pipe flow stability.

Reverting to the case at hand, eigenfunction H for wave number $n = 0$, we note that the program of Ref. 6 was rewritten for this case, incorporating the newly formulated boundary conditions of Ref. 9. In addition, a new, generalized stability criteria was adopted. Moreover, a new technique was introduced which allows the use of nonuniform meshes to reduce computational time.

Lastly, two data reduction programs were written to process data produced by the main investigative program.

II. THE VORTICITY TRANSPORT EQUATION

Although a complete treatment of this subject is contained in Appendix A of Ref. 4 and further addressed in Ref. 6 and Ref. 9, it is felt that a brief overview is still required here to maintain continuity with previously referenced works. This discussion is an abbreviated version of Section II of Ref. 6.

Laminar flow of an incompressible fluid of constant viscosity is governed by the Navier-Stokes equation and the continuity equation. Taking the curl ($\nabla \times$) of the Navier-Stokes equation and introducing a perturbation velocity (\bar{v}) and vorticity ($\bar{\omega}$) gives the vorticity transport equation which is equation (A-10) of Appendix A, Ref. 4.

Expressing this equation in terms of the complex velocity vector potential, \bar{W} , gives

$$W(x, r, \theta, t) = (\bar{e}_x F(r) + \bar{e}_r G(r) + \bar{e}_\theta H(r)) e^X \quad (2-1)$$

where

$$X = \alpha x + \beta \theta + \gamma t \quad (2-2)$$

and

$$\bar{v} = \nabla \times \bar{W} \quad (2-3)$$

$$\bar{\omega} = \nabla \times \bar{v} . \quad (2-4)$$

It should also be noted that, as shown in part one of Appendix G in Ref. 4, α and γ are complex while β is a purely imaginary quantity defined by

$$\beta = i n \quad n = 0, 1, 2, \dots \quad (2-5)$$

When expressed in the form of equation (2-1), the vorticity transport equation becomes three simultaneous fourth-order differential equations of the form

$$\begin{aligned} & [M_4] \begin{Bmatrix} D^4 F \\ D^4 G \\ D^4 H \end{Bmatrix} + [M_3] \begin{Bmatrix} D^3 F \\ D^3 G \\ D^3 H \end{Bmatrix} + [M_2] \begin{Bmatrix} D^2 F \\ D^2 G \\ D^2 H \end{Bmatrix} \\ & + [M_1] \begin{Bmatrix} DF \\ DG \\ DH \end{Bmatrix} + [M_0] \begin{Bmatrix} F \\ G \\ H \end{Bmatrix} - \gamma ([N_2] \begin{Bmatrix} D^2 F \\ D^2 G \\ D^2 H \end{Bmatrix} \\ & + [N_1] \begin{Bmatrix} DF \\ DG \\ DH \end{Bmatrix} + [N_0] \begin{Bmatrix} F \\ G \\ H \end{Bmatrix}) = \begin{Bmatrix} 0 \\ 0 \\ 0 \end{Bmatrix} \end{aligned} \quad (2-6)$$

Equations (2-5) may be further expressed in the abbreviated form

$$\bar{\Gamma} = \begin{Bmatrix} \bar{\Gamma}_x \\ \bar{\Gamma}_r \\ \bar{\Gamma}_\theta \end{Bmatrix} = \begin{Bmatrix} 0 \\ 0 \\ 0 \end{Bmatrix} \quad (2-7)$$

where $\bar{\Gamma}$ appears to be a set of three coupled equations in the components of \bar{W} . As given in Appendix B of Ref. 4, equations (2-7) actually represent only two independent conditions and by an appropriate linear combination of Γ_x and Γ_θ , equations (2-6) can be expressed as a set of two equations in three unknowns. The appropriate linear combination is given in Appendix B of Ref. 4 and yields the set of equations

$$\begin{aligned} \Gamma_r &= 0 \\ -\frac{in}{r} \Gamma_x + \alpha \Gamma_\theta &= 0 . \end{aligned} \quad (2-8)$$

Except for the case where n is equal to zero, equations (2-8) do not uncouple. The linear combination given by the second of equations (2-8) does, however, reduce the highest order derivative of $G(r)$ in equations (2-6) to second order. Appendix C of Ref. 4 illustrates the redundancy of the three components of \bar{W} , allowing one of these components to be arbitrarily set to zero for all r . The maximum benefits of equations (2-8) are obtained if

$$F(r) = 0 \quad (2-9)$$

Incorporating equations (2-8) and (2-9) into equations (2-6) results in the form

$$\begin{aligned}
 & [M'_4] \begin{Bmatrix} D^4 G \\ D^4 H \end{Bmatrix} + [M'_3] \begin{Bmatrix} D^3 G \\ D^3 H \end{Bmatrix} + [M'_2] \begin{Bmatrix} D^2 G \\ D^2 H \end{Bmatrix} \\
 + & [M'_1] \begin{Bmatrix} DG \\ DH \end{Bmatrix} + [M'_O] \begin{Bmatrix} G \\ H \end{Bmatrix} - \gamma ([N'_2] \begin{Bmatrix} D^2 G \\ D^2 H \end{Bmatrix} \\
 + & [N'_1] \begin{Bmatrix} DG \\ DH \end{Bmatrix} + [N'_O] \begin{Bmatrix} G \\ H \end{Bmatrix}) = \begin{Bmatrix} 0 \\ 0 \end{Bmatrix} \quad (2-10)
 \end{aligned}$$

where the coefficient matrices are given by equations (2-10) through (2-17) of Ref. 6. It is appropriate to note that these same coefficient matrices appear in Ref. 9, equations (A1) through (A9), in a slightly different form resulting from the substitutions

$$U = 2(1 - r^2) \quad (2-11)$$

$$t = \alpha^2 + \frac{\beta^2}{r^2} \quad \text{and} \quad (2-12)$$

$$T = \alpha U - \frac{1}{R_e} \left(\alpha^2 + \frac{\beta^2}{r^2} \right) . \quad (2-13)$$

As discussed in the previous section, the case where

$$\beta = \text{in} , \quad n = 0 \quad (2-14)$$

leads to great simplifications in equations (2-10), (2-12) and (2-13). In particular, equations (2-10) uncouple and allow an independent investigation of either H or G . As a result of the findings discussed in Section I, it was decided to explore the function H only. This reduced equation (2-10) to that of equation (A-6) of Appendix A, which is a linear, homogeneous fourth order differential equation in $H(r)$.

III. NUMERICAL METHODS

Substituting the change of variable $H = rQ$ as given in equation (A-1) and the coefficients defined in equations (A-11) through (A-18) into the vorticity transport relation, equation (A-6), gives the expression

$$\begin{aligned} M_4 D^4 Q + M_3 D^3 Q + M_2 D^2 Q + M_1 DQ + M_0 Q \\ - \gamma [N_2 D^2 Q + N_1 DQ + N_0 Q] = 0 , \end{aligned} \quad (3-1)$$

which is a homogeneous fourth order differential equation in $Q(r)$. The boundary conditions for this case are derived in detail in Ref. 9 as

$$\begin{aligned} Q(1) &= 0 \\ DQ(1) &= 0 \\ DQ(0) &= 0 \\ D^3 Q(0) &= 0 . \end{aligned} \quad (3-2)$$

The boundary finite difference equations derived in Appendix B from equations (3-2), along with the standard central difference equations given in Ref. 6, allow the function $Q(r)$ to be approximated by a finite number of discrete unknowns. As shown by Figure 3-1 below, the non-dimensionalized radius of the pipe is divided into a one-dimensional

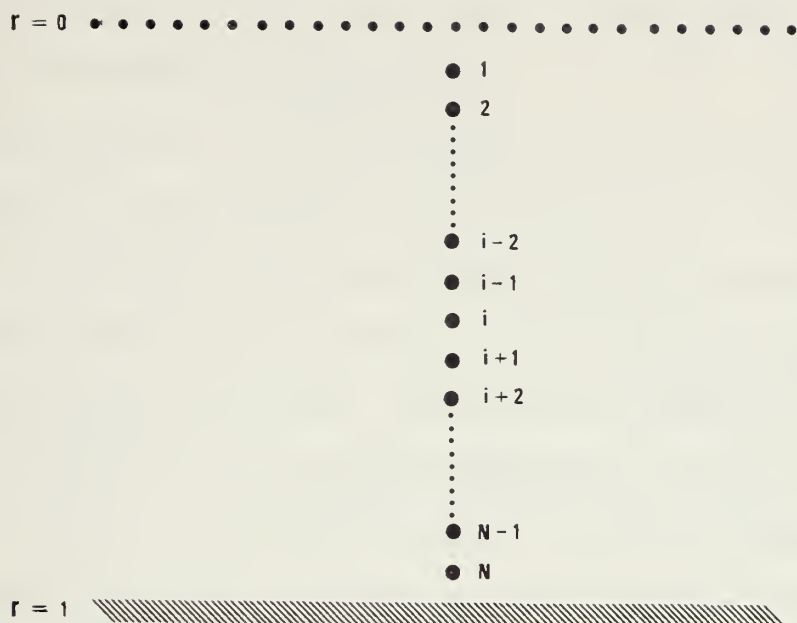


Figure 3-1 Finite Difference Mesh

computational mesh consisting of N interior points, $N+1$ intervals, and $N+2$ total points, including the boundary points at $r = 1$ and $r = 0$. As will be discussed later, the spacing between these points may or may not be uniform. For the uniform case, the spacing is defined by

$$\delta = 1/(N+1) . \quad (3-3)$$

For the nonuniform case, a change of independent variable is performed. The spacing of the new independent variable, η , is still given by equation (3-3).

With a nonuniform mesh, the points shown in Figure 3-1 will be concentrated near the axis or near the wall according

to the type of offset specified. These effects are discussed in detail in Section IV.

Substitution of the finite difference equations of Appendix B into equation (3-1) results in a set of N , linear, algebraic difference equations in terms of the unknown value of Q at each of the N interior points of the computational mesh. Since each of these equations is of the form of a linear combination of the i th, central, point and the two, three or four adjacent points (depending on the order of the derivative being approximated), this system of equations consists of a coefficient array multiplying a vector containing the unknown value of the function Q at each of the N interior points. This technique allows the problem to be converted into an eigenvalue problem of the form

$$[X] \{Q\} - \gamma[Y] \{Q\} = 0 \quad (3-4)$$

with the basic composition of the arrays $[X]$ and $[Y]$ and the vector $\{Q\}$ as illustrated in Figure 3-2 below.

It should be noted at this point that Figure 3-2 differs somewhat from the normal finite difference banded matrix in the first two rows and last row because of the method of deriving the finite difference approximations at the boundaries. Additionally, the order of the N unknowns has been reversed from that of Ref. 6. This was done to conform to standard matrix notation.

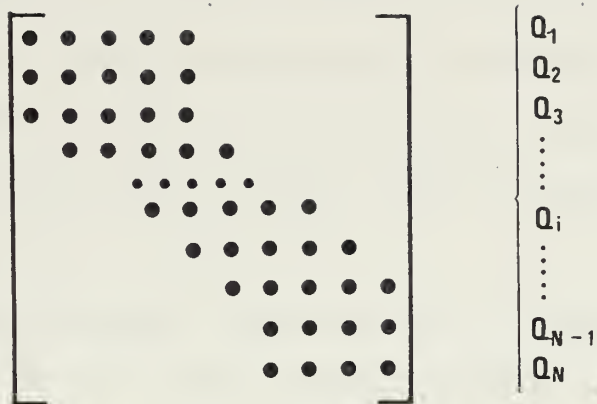


Figure 3-2 Basic Composition of Coefficient Arrays and Vector of Unknowns

This array is established by the subroutine MSET2 in conjunction with the subroutine MSET1 and function subprograms CQM1E1 and CQM2E1, which compute the numerical value for each element in the array. Subroutine MSET1 provides the coefficients given by equations (A-11) through (A-18) of Appendix A or by equations (C-24) through (C-31) if a nonuniform mesh is specified. Function CQM1E1 then computes the values for each of the elements of array [X] in equation (3-4) using the coefficients passed from subroutine MSET1 in vector CQM1. Function subprogram CQM2E1 performs the same function for matrix [Y] in equation (3-4) using the coefficients passed in vector CQM2.

The solution of the eigenvalue problem as formulated to this point is carried out by the controlling subroutine of program PIPE0, subroutine STAB, by the following steps:

- 1) Subroutine MSET2 is called twice to set up the coefficient matrices [X] and [Y] of equation (3-4).

- 2) Subroutine CDMTIN is then called to invert matrix $[Y]$, the second coefficient array in equation (3-4). CDMTIN was obtained from the IBM Library routine CMTRIN by modifying it to accept double precision arrays.
- 3) Both coefficient arrays, $[X]$ and $[Y]$, are then pre-multiplied by $[Y]^{-1}$. Since multiplication of an array by its inverse invariably results in the identity matrix, $[I]$, only the product $[Y]^{-1}[X]$ is computed using subroutine MULM. This converts the eigenvalue problem of equation (3-4) to the more conventional form

$$([Z] - \gamma[I])\{Q\} = 0 \quad (3-5)$$

where

$$[Z] = [Y]^{-1}[X] \quad (3-6)$$

- 4) Since all programs currently available for solving equations (3-5) require that the real and imaginary parts of the elements of $[Z]$ be presented in separate arrays, subroutine DSPLIT is called to accomplish this.
- 5) The eigenvalues and eigenvectors of equations (3-5) are computed using subroutines EBALAC, EHESSC, ELRH2C and EBBCKC which are available through the International

Math and Statistics Library. Subroutine EBALAC balances matrix $[Z]$ by equalizing the exponents of all terms. The details of this transformation are retained for later use. The balanced matrix is then passed to subroutine EHSSC where it is reduced into the complex upper Hessenberg form. Subroutine ELRH2C then solves for the eigenvalues and eigenvectors. To transform the eigenvectors back into the original unbalanced form, EBBCKC is finally called using information passed from subroutine EBALAC.

For each solution, subroutine STAB determines the least stable eigenvalue (largest algebraic value) and then writes the values of N , R_e , α_R , α_I , λ , γ_{RL} , γ_{IL} and KSET to file FT02F001. The eigenvector corresponding to the least stable eigenvalue is also written to FILE FT02F001 when MODENO is set equal to one.

Control of subroutine STAB is accomplished by the main program, PIPE0. This program is a time-sharing (CP/CMS) program. Modes one and three compute the stability of the flow for a given set of input conditions. Mode one writes the least stable eigenvector to FILE FT02F001 while this output is inhibited when MODENO is set equal to three. To generate data for program EIGFCN, program PIPE0 must be run with MODENO equal to one.

Mode two operation generates a grid of stability values (stability map) based on parameters read in from FILE FT01F001. Due to the long run time in this mode, only small meshes can be generated under CP/CMS. Longer runs must be accomplished under batch, with changes to the program as specified in the comments section. Data is output to file FT03F001 when MODENO is equal to two and is compatible with program STBCONT.

The plotting programs EIGFCN and STBCONT were used to process the data generated by program PIPE0 in modes one and three, respectively. Program EIGFCN generates normalized plots of the perturbation velocity, u , as a function of radius, r . The perturbation velocities generated in accordance with Appendix D were normalized in two steps. First the perturbation velocity of largest magnitude was determined. Letting this velocity be termed u_C , a normalizing constant producing unit magnitude and zero phase angle in u_C was found in the following manner:

If

$$u_C = u_{RC} + iu_{iC} , \quad (3-7)$$

then

$$Cu_C = 1 + i(0) \quad (3-8)$$

where C is the normalizing constant. Thus,

$$C = \frac{1}{u_{RC} + iu_{iC}} = \frac{u_{RC} - u_{iC}}{(u_{RC}^2 - u_{iC}^2)} \quad (3-9)$$

$$= \frac{\bar{u}_C}{|u_C|^2} \quad (3-10)$$

where \bar{u}_C is the complex conjugate of u_C .

The nondimensionalized radius values were taken directly from the data cards for uniform meshes or computed from equations (C-32) or (C-40) in the case of a nonuniform mesh.

Program STBCONT plots the stability contours against α_R and α_I . The stability map generated by program PIPE0 is searched columnwise and rowwise for sign changes for each of the three stability criteria discussed in Section V and Ref. 9. The points are then plotted, producing contours of incipient, critical and fully developed instability and areas that denote stable flow and subcritical, supercritical and hypercritical instability.

Both programs, EIGFCN and STBCONT, utilize the NPS VERSATEC plotter, certain built-in VERSATEC subroutines, and subroutine PLOTG. These routines are only accessible when running under FORTCLGW.

IV. RESULTS

A. STABILITY

Since an understanding of the term stability is necessary to interpret the results of this investigation, a brief discussion is presented here. A complete discussion of the generalized criteria of stability is given by Gawain [9].

The characteristics of the flow for the case $n = 0$ are set by the parameters R_e and α . For fixed values of these parameters, the solution of equations (3-5) is a set of N eigenvalues, γ , and their corresponding eigenvectors, Q . As can readily be seen from equation (2-1), the value of the real part of the complex eigenvalue γ will determine the growth or decay rate in time of the perturbation. Since positive values of the real part of γ represent an exponential growth rate in time, the most important γ is the one having the largest algebraic value for its real part. This root is termed the least stable root and will be represented by the symbol γ_{RL} . As the stability represented by γ_{RL} is that seen by a fixed observer, it is not the most general criterion. As derived in Ref. 9, a more appropriate stability criterion is that based on an axis system moving at the average volumetric velocity of the flow. This criteria is termed γ_{RL}^* and is defined by Ref. 9 as

$$\gamma_{RL}^* = \gamma_{RL} + \alpha_R . \quad (4-1)$$

For this and subsequent discussions, the subscript will be dropped and γ^* will refer to the quantity defined by equation (4-1). Three stability cases arise from this equation. The first is termed incipient instability and is defined by

$$\gamma^* = -|\alpha_R| . \quad (4-2)$$

The second case, termed critical instability, is given by

$$\gamma^* = 0 \quad (4-3)$$

and, lastly, the case termed fully developed instability is said to exist when

$$\gamma^* = +|\alpha_R| . \quad (4-4)$$

The transition from stable flow to fully developed instability is progressive and several distinct stages are given in Ref. 9 to describe this transition. The region from incipient to critical instability is termed subcritical instability, that from critical instability to fully developed instability is called supercritical instability while that beyond fully developed instability is termed hypercritical instability.

B. PERTURBATION VELOCITY PLOTS

Initial investigation of the function Q was centered around plotting its appearance in the region of interest. A Reynolds number of 1150 (2300 based on diameter) was chosen as this value is generally accepted as the nominal value for transition to turbulent flow. The value of α was set at $-0.5 + i 10.0$ for the major part of the investigation as preliminary checks revealed that supercritical instabilities were present for this value. A secondary Reynolds number of 4000 was chosen to show trends.

The quantity chosen as the most realistic and representative of the eigenfunction Q is the axial perturbation velocity, u . This quantity was derived from the elements of the least stable eigenvector as outlined in Appendix D. Initially, R_e and α_I were held fixed and α_R was varied over a range of positive and negative values. For values of α_R below about two, the normalized perturbation velocity was found to have all activity near the axis with a decay essentially to zero by $r = 0.3$. A typical plot of u versus r for an α_R in this range is shown in Figure 4-1. When α_R was made sufficiently positive, the plot changed significantly in both appearance and region of activity. Figure 4-2 shows a plot of u for $\alpha_R = 2.5$. The activity can now be seen to be concentrated near the wall, with most of the activity occurring at r values greater than 0.7.

Although no particular relationship between the nature of u and the stability of the flow was evident or expected,

the plots were nevertheless valuable as indicators for various parameters involved in the investigation.

First, as can be seen by the differences in Figures 4-1 and 4-2, the plots were ideal indicators of changes in the nature of the function Q . Secondly, the adequacy of the mesh could be directly observed by noting the number of points defining the curves in regions of high activity. Figures 4-3, 4-4 and 4-5 show the same conditions as Figure 4-1 but with decreasing number of mesh points, N . Lastly, the effects of nonuniform meshes could be observed as will be discussed later in this section.

C. STABILITY CONTOUR PLOTS

The principal results of this investigation are shown in Figures 4-6 and 4-7. Although these two figures pertain to only a limited portion of the complex α plane, they do represent a significant advance in the investigation of pipe flow stability. As can be seen in these figures, the flow is characterized by regions of differing stability, ranging from stable through supercritical instability. Note that these two figures correspond to Reynolds numbers of 1150 and 4000, respectively. This is a result that has not, to this writer's knowledge, been heretofore achieved by a linearized analysis of fully developed pipe flow. The figures also show that, as has been born out by previous investigations, flow for purely sinusoidal oscillations ($\alpha_R = 0$) is stable. Additionally, a comparison of Figures 4-6

and 4-7 shows the effect of Reynolds number on the flow stability. It is clear from this comparison that an increase in Reynolds number reduces the size of the stable regions in the complex α plane; in other words, stability decreases with increasing Reynolds number. This trend agrees with our general experience pertaining to fluid flow. Lastly, the effect of the real and imaginary parts of the wave number α can readily be seen. For α_R , increasingly negative values produce successively greater levels of instability. While a contour plot was not produced for positive values of α_R , point checks of stability in this region suggest that somewhat similar contours exist in the right half-plane also. For α_I , increasing values produce increasing stability. This effect is also more pronounced at the lower Reynolds number.

D. NONUNIFORM MESH EFFECTS

One of the difficulties in this investigation was the relatively long computing time required to obtain an accurate solution, especially when operating under CP/CMS (time-sharing). The major factor controlling computing time was the number of interior mesh points, N . As an example, an increase in N of 50 percent resulted in a fourfold increase in computing time. Therefore, the desired objectives of rapidity and accuracy were in direct conflict. Additionally, follow-on investigations for values of angular wave number n other than zero involve matrices twice the order required for this case because of the coupling of equations (2-8).

For these reasons, a nonuniform mesh was developed to obtain increased accuracy at lower values of N . The nature of the velocities as seen in Figures 4-1 and 4-2 shows that a high degree of resolution in the computational mesh is only required in the vicinity of the axis (α_R less than about 2) or the wall (α_R greater than about 2). It was therefore theoretically possible to redistribute the points at moderate values of N to attain resolutions equivalent to much finer (and more time-consuming) uniform meshes.

As can be seen from Figures 4-8 and 4-9, the value of γ^* varies with the number of mesh points, N . Theoretically, each of these curves would approach some limiting value if N were increased without bound, and it is this theoretical limit that represents the required solution. In practice, it is adequate to approximate the unknown limit by a point that lies on the relatively flat portion of the curve at a value of N which is practically attainable and which does not involve a prohibitively long computing time. It has been found in this investigation that $N = 79$ fulfills these conditions.

The conversion to a nonuniform mesh involved a change of independent variable and the introduction of an analytical function to control the distribution of the mesh points. The details of these steps are given in Appendix C. By varying the mesh offset parameter, λ , it was possible to vary γ^* over a wide range. To determine when the high

accuracy solution ($N = 79$) and the nonuniform solutions were approximately equal, γ^* was plotted versus λ for fixed values of R_e , α and N with the value of γ^* for $N = 79$ as a reference. Figure 4-10 shows a plot of this type for $N = 31$. The appropriate value of λ can be seen to be approximately 1.1. Figure 4-11 is the perturbation velocity plot of the solution for $N = 31$ and $\lambda = 1.1$ for the same R_e and α as Figure 4-1. Note that the γ^* values are equal for these two figures. While the resolution of Figure 4-11 is not quite as fine as that of Figure 4-1, a comparison of Figure 4-11 with Figure 4-5 makes the improved resolution obvious. Figures 4-2 and 4-12 are similar to Figures 4-1 and 4-11 except that a wall offset was used. Note that for this case $\lambda = 1.2$, which points to a drawback of the nonuniform mesh, that of dependence on input conditions. While a check of λ dependence on α was not made, it most probably exists. There is also, however, the possibility that for small regions of the complex α plane, the variations in λ are small enough to allow an average value of λ to be nearly optimum for the entire region. While not used for the main results of this study, the method as developed here may well prove to be of maximum utility in follow-on investigations of higher angular wave numbers.

E. NUMERICAL ACCURACY

To ensure that the solutions presented here were of sufficient accuracy, two separate checks were made. The

first, γ^* dependence on N , is the most commonly used criterion.

For a solution to be accurate, it should be virtually independent of mesh fineness, that is, of N . The required magnitude of N for an accurate solution was found by plotting γ^* against N . Figures 4-8 and 4-9 both show that the solution is well converged for $N = 79$ at Reynolds numbers of 1150 and 4000, as γ^* changes by only .001 to .003 from $N = 31$ to $N = 79$ for both values of Reynolds number.

The second verification of the solution, so obvious that it is sometimes overlooked, involves simply substituting the numerical solution (least stable eigenvector) into the governing equation to ensure that it is indeed being satisfied. A short program was independently written to check the finite difference representations of equation (3-1) at the first and last interior stations and at a mid-radius station. Initial checks of numerical solutions yielded unsatisfactory results and led to the discovery of various programming errors. In particular, it was discovered that four double precision constants in the finite difference approximations were lacking the required "D0" exponent. Elimination of these seemingly trivial errors resulted in a surprising four order-of-magnitude improvement in the accuracy of the solution, with the left side of equation (3-1) improving from order 10^{-4} to order 10^{-8} .

It is instructive to note at this point that the order of magnitude of the left side of equation (3-1) is not the

true measure of its satisfaction. A more correct procedure is to compare this value with the largest term in the equation. When examined from this viewpoint, the relative error for solutions at $R_e = 1150$ and $R_e = 4000$ are found to be of order 10^{-11} to 10^{-12} , a very satisfactory result.

Therefore, by these results, the solutions presented here are both virtually independent of N and satisfy the governing differential equation to a high degree. The efforts expended to reach these conclusions were well worth the result and also point out that attention to detail is fundamental to accurate numerical results.

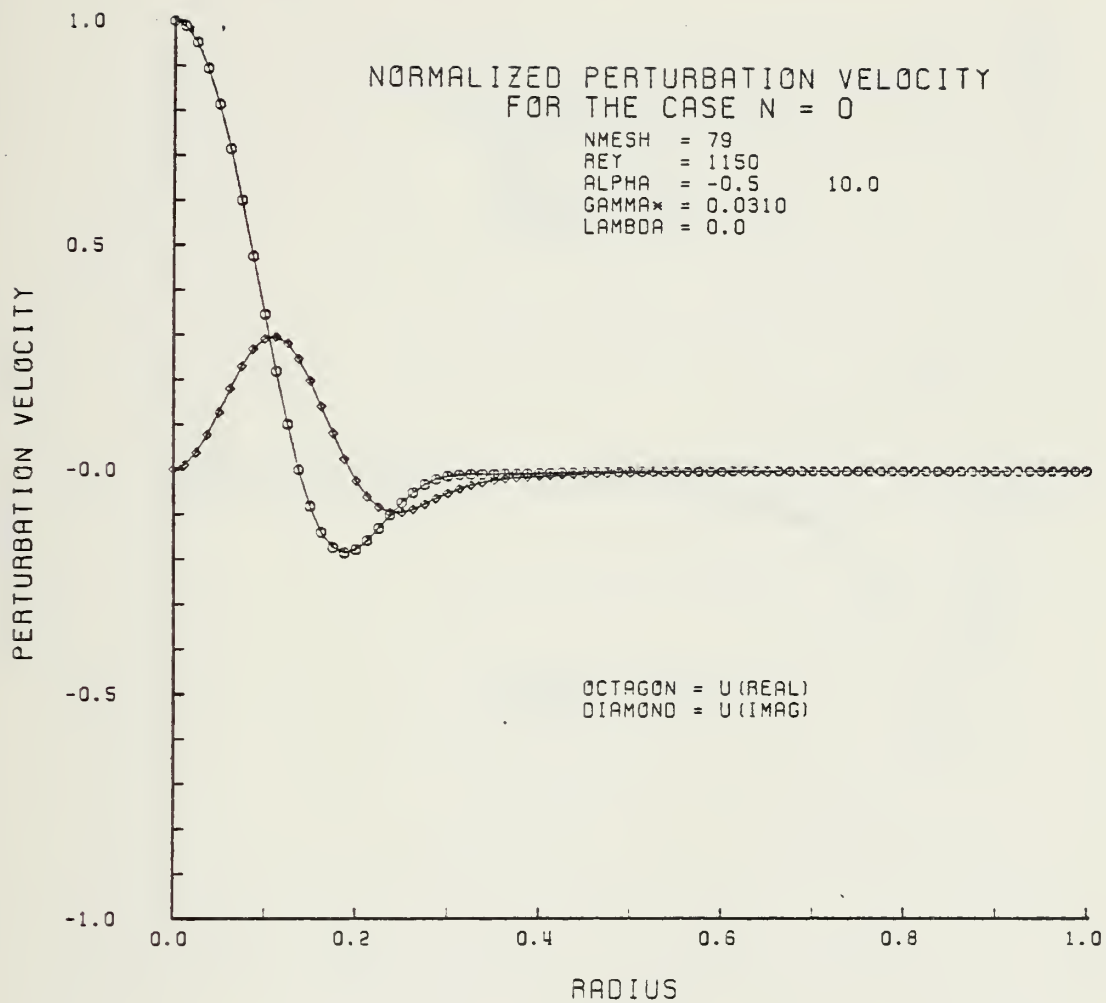


FIGURE 4-1

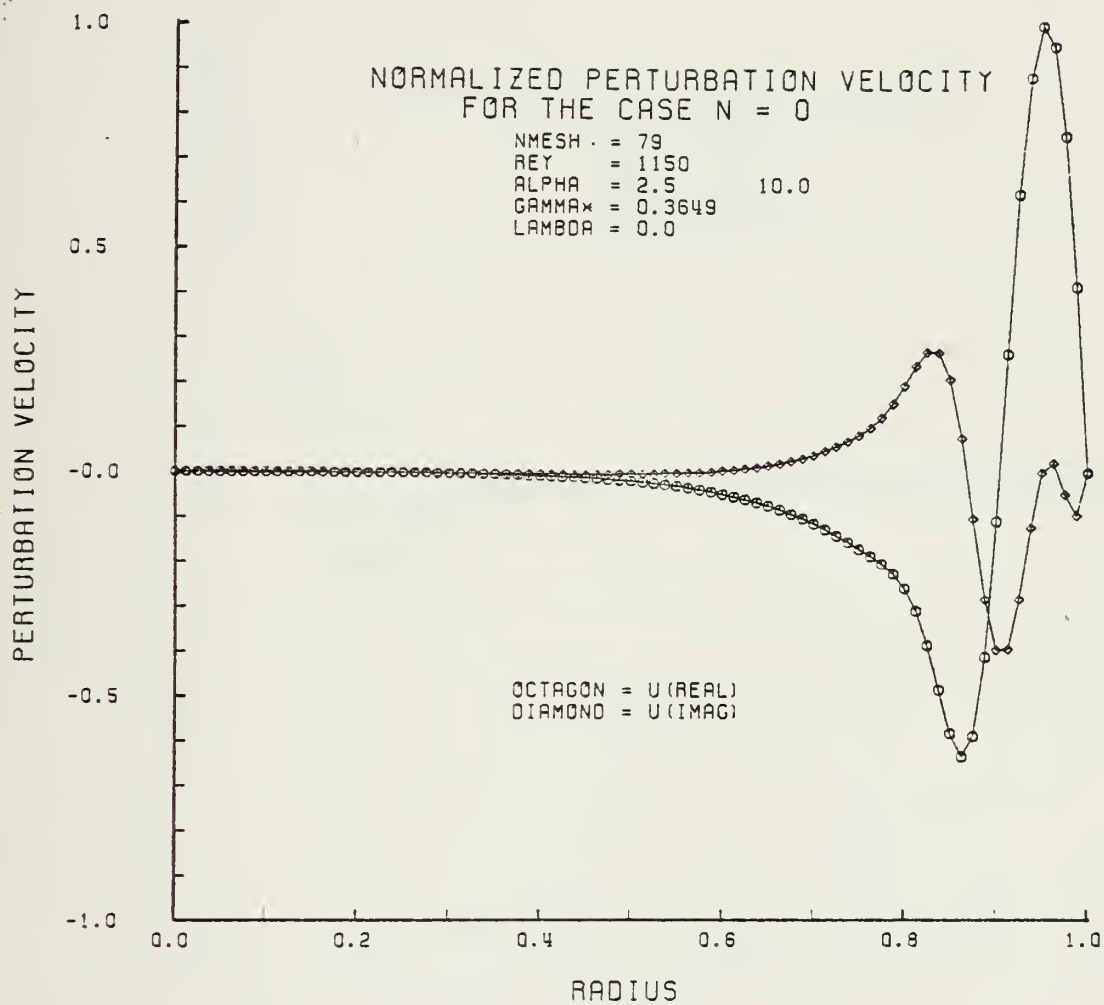


FIGURE 4-2

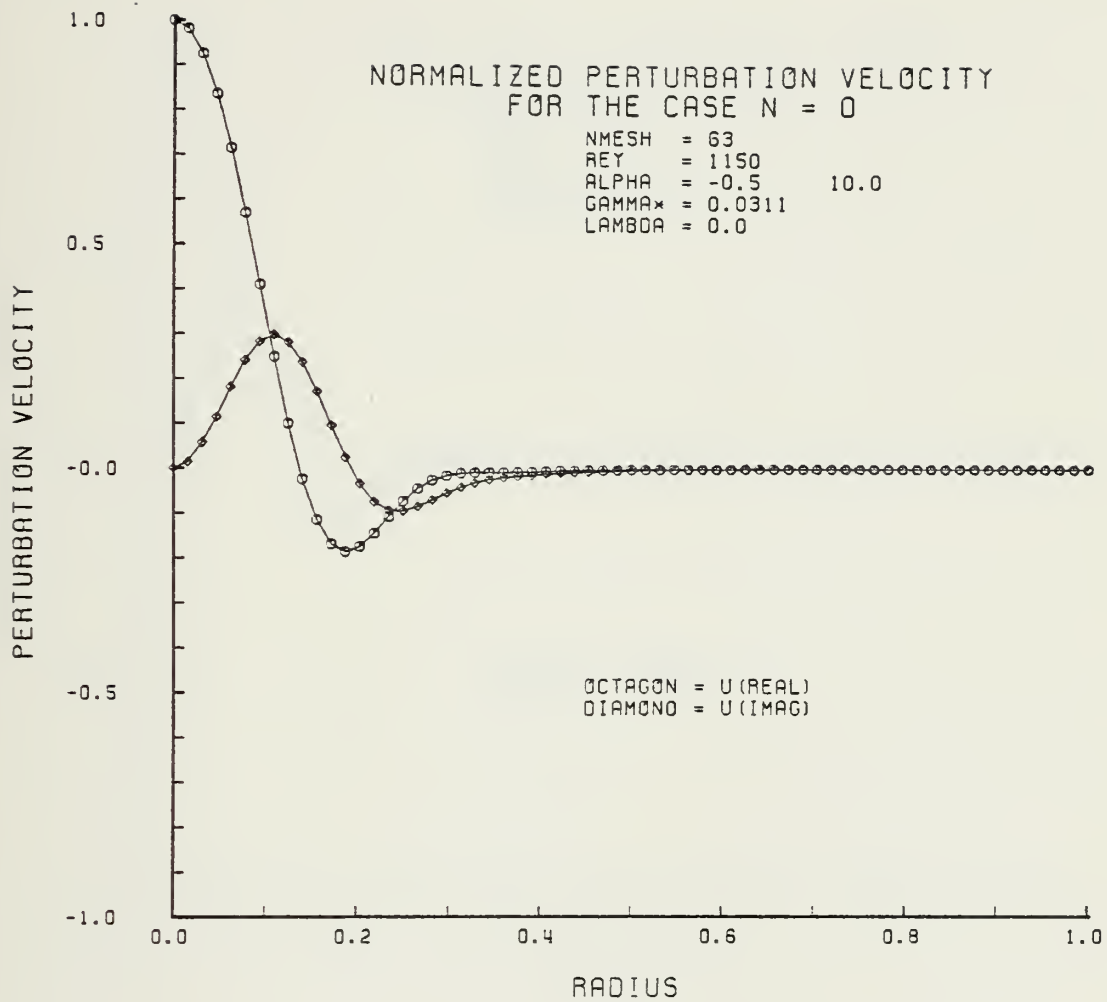


FIGURE 4-3

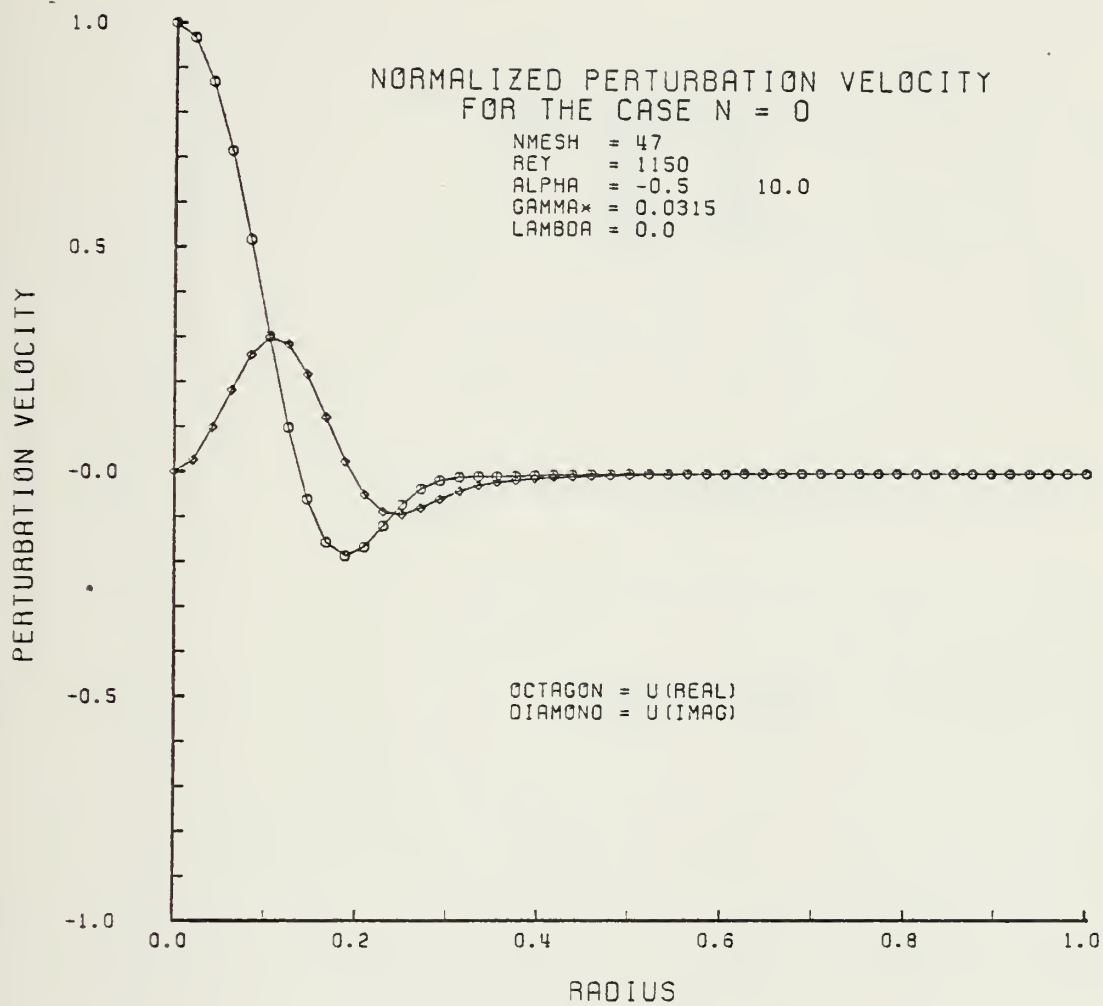


FIGURE 4-4

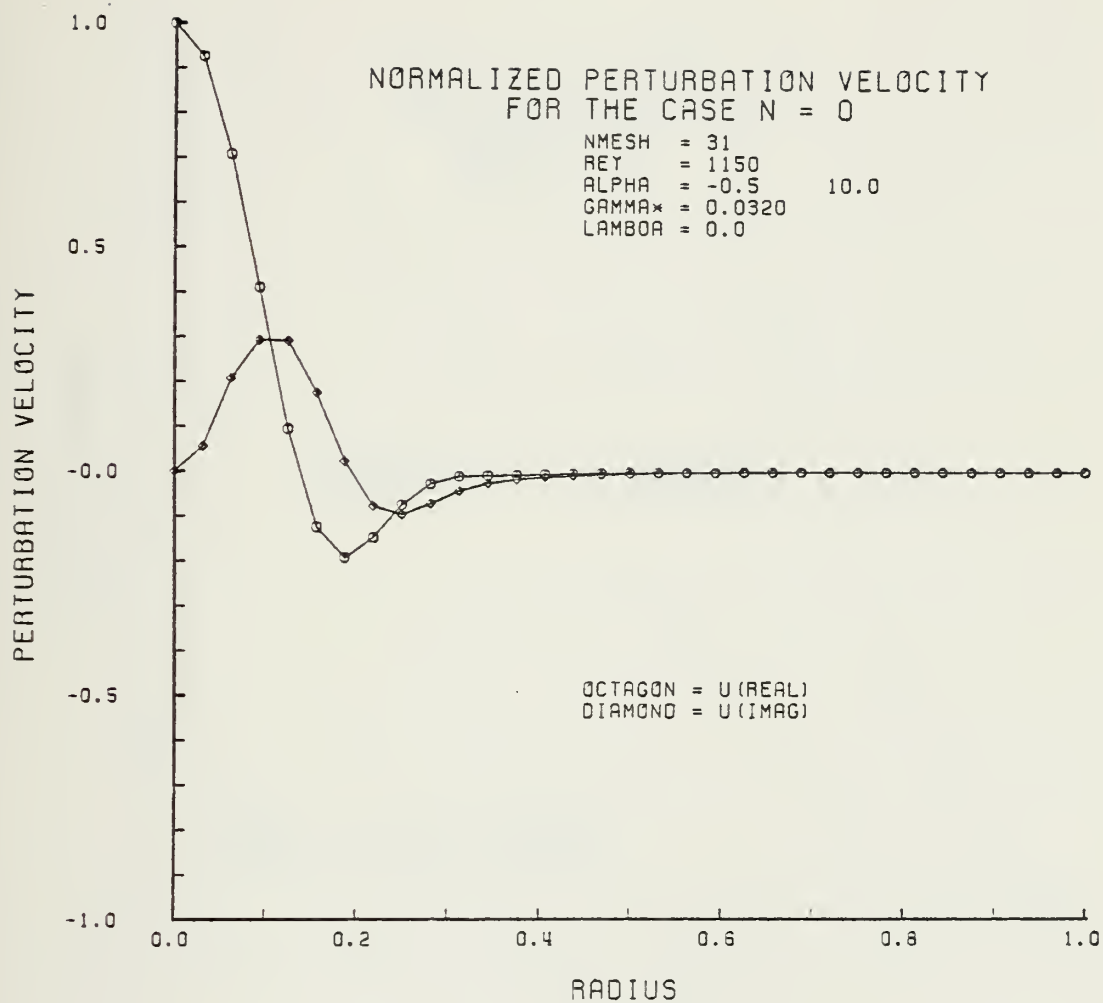


FIGURE 4-5

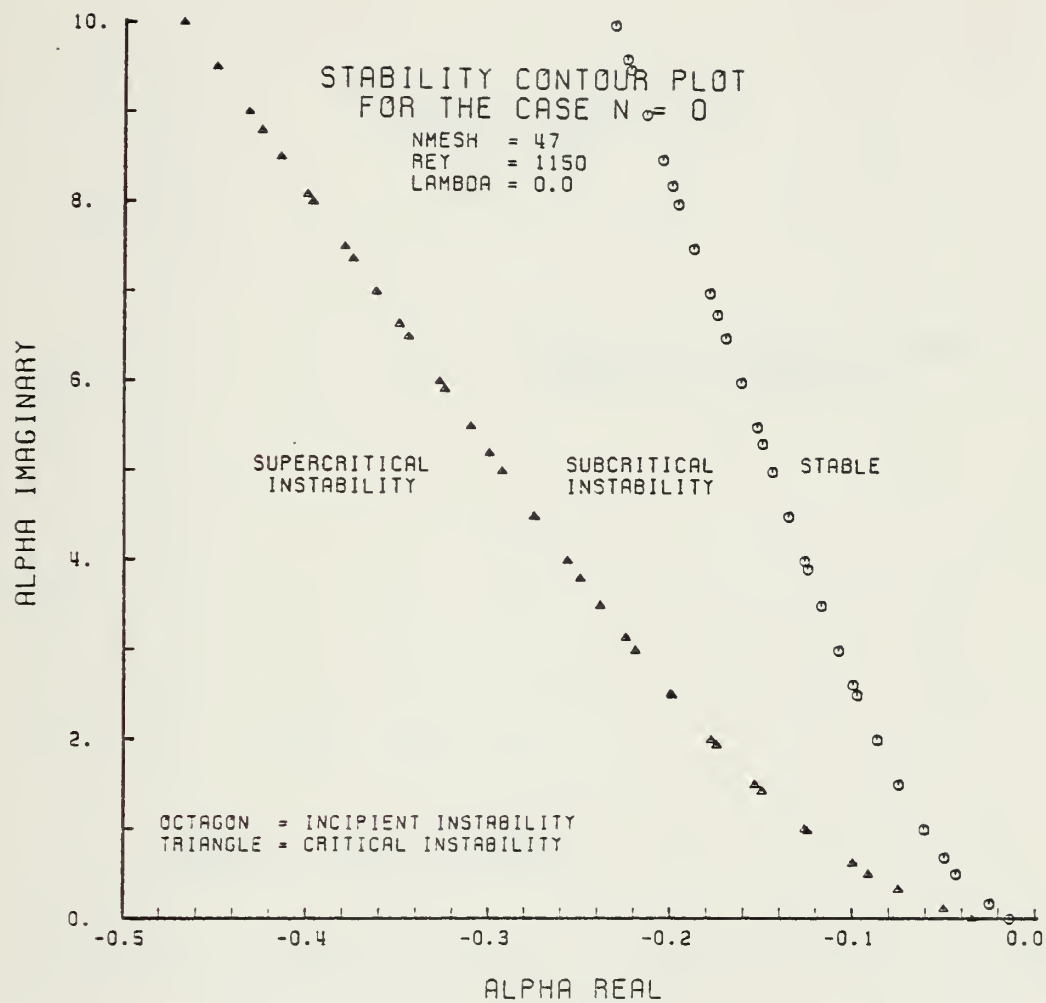


FIGURE 4-6

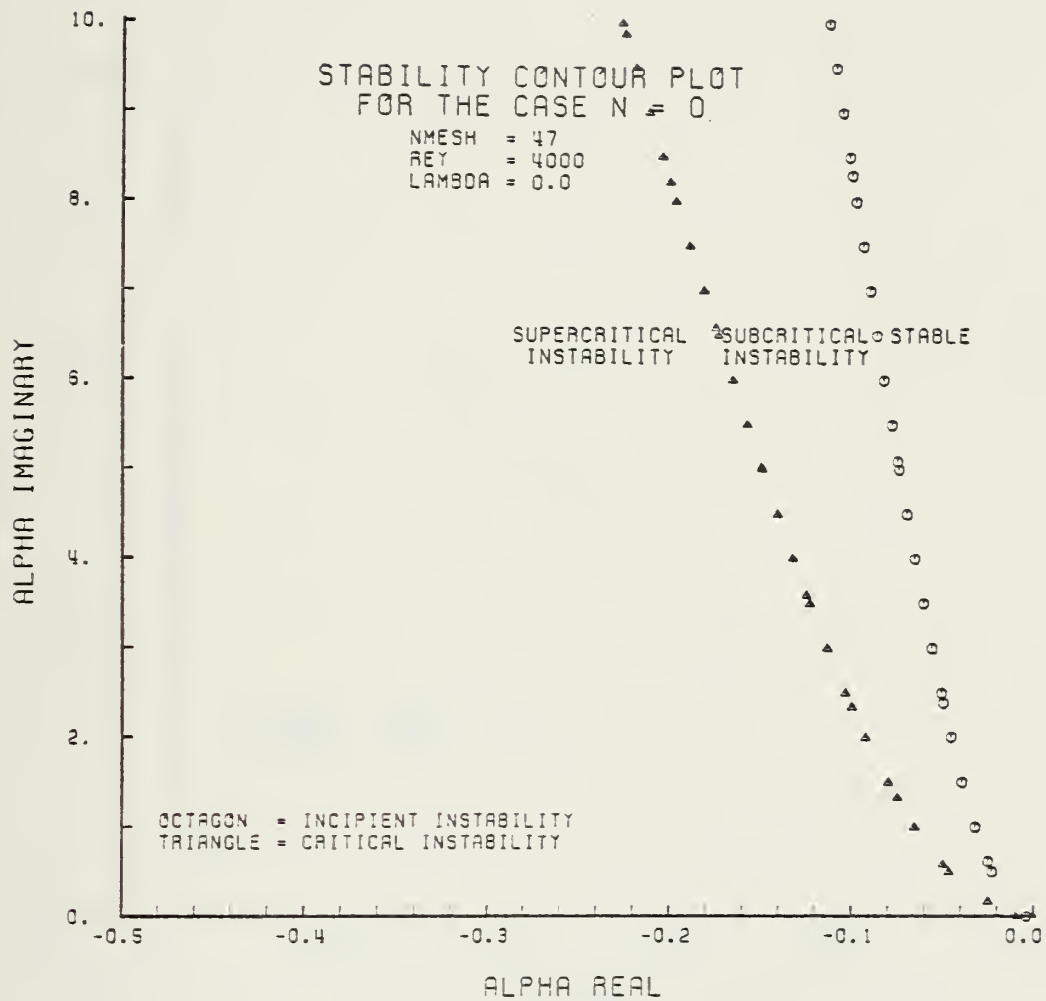


FIGURE 4-7

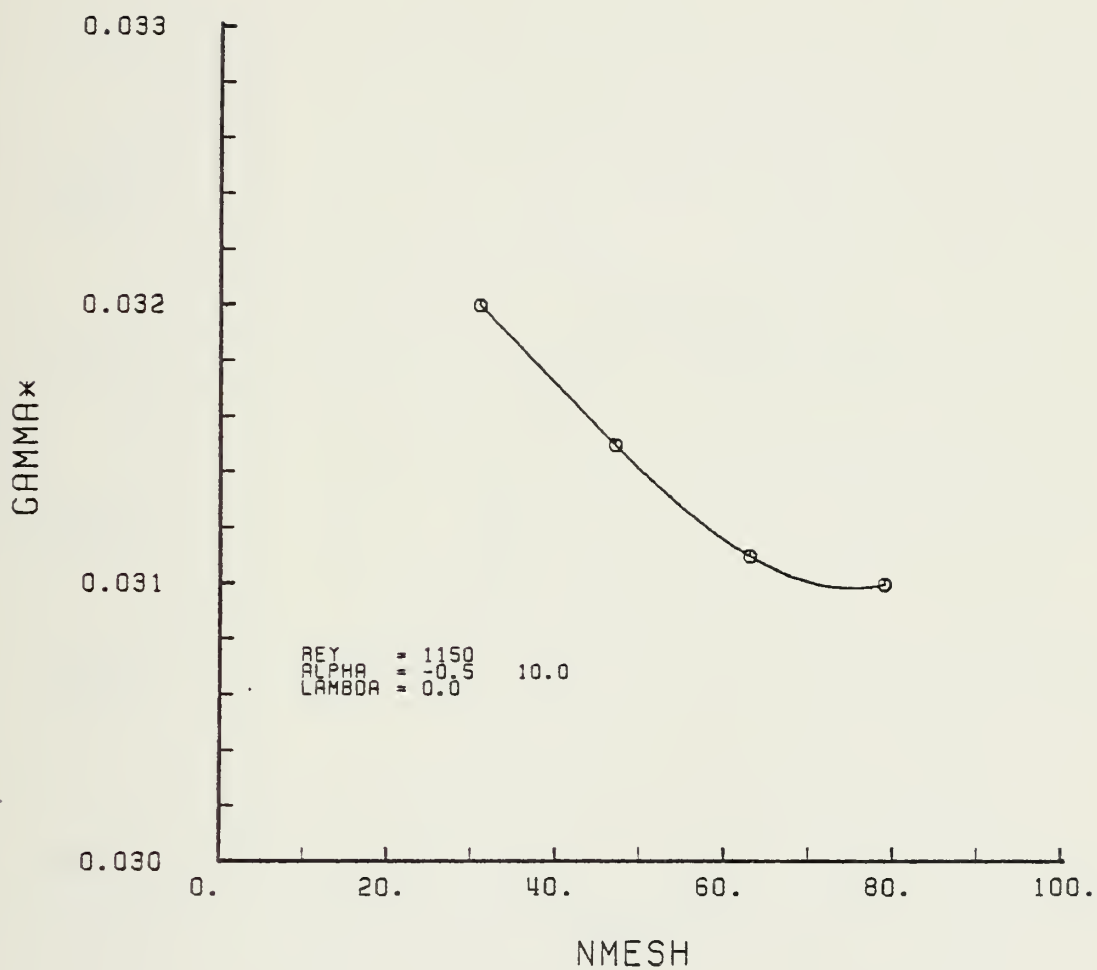


FIGURE 4-8. γ^* Versus Number of Mesh Points, N.

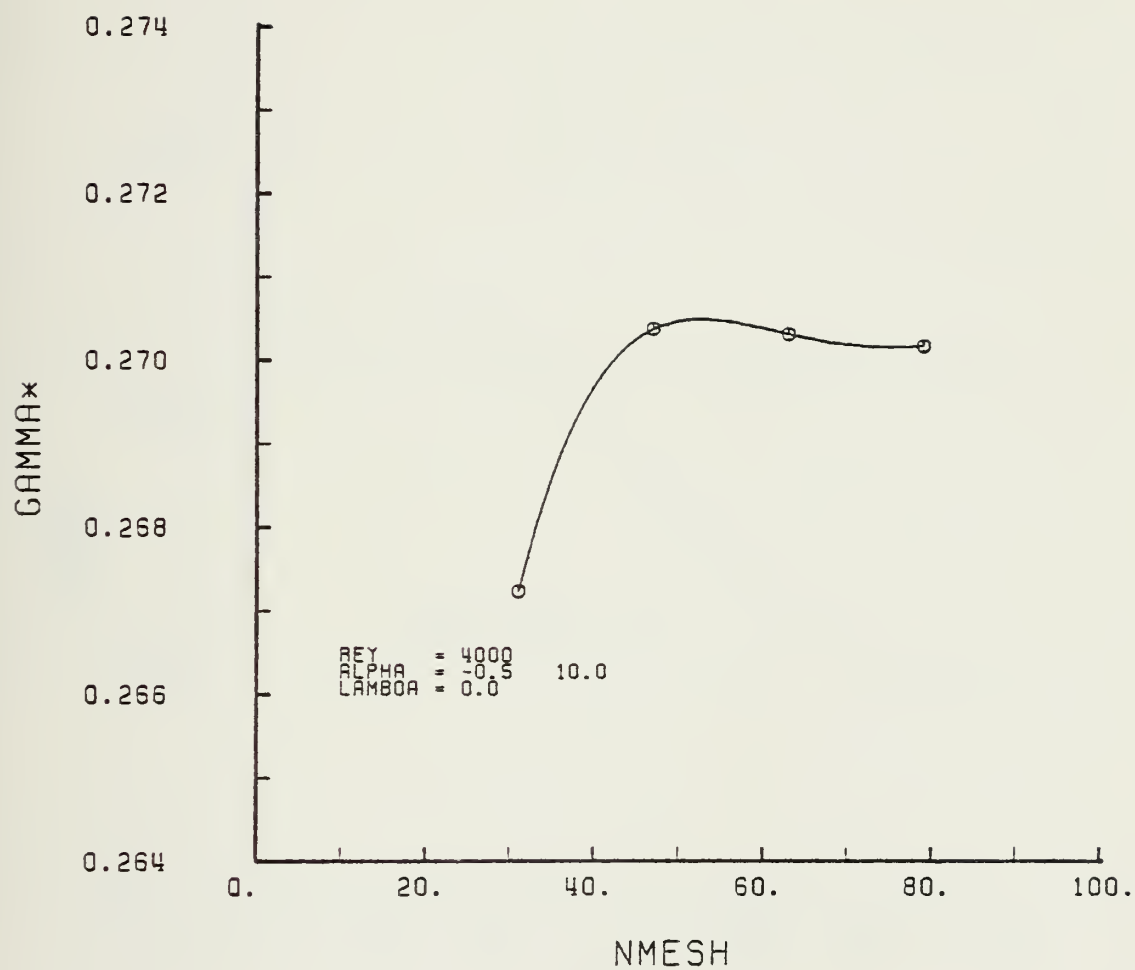


FIGURE 4-9. γ^* Versus Number of Mesh Points, N.

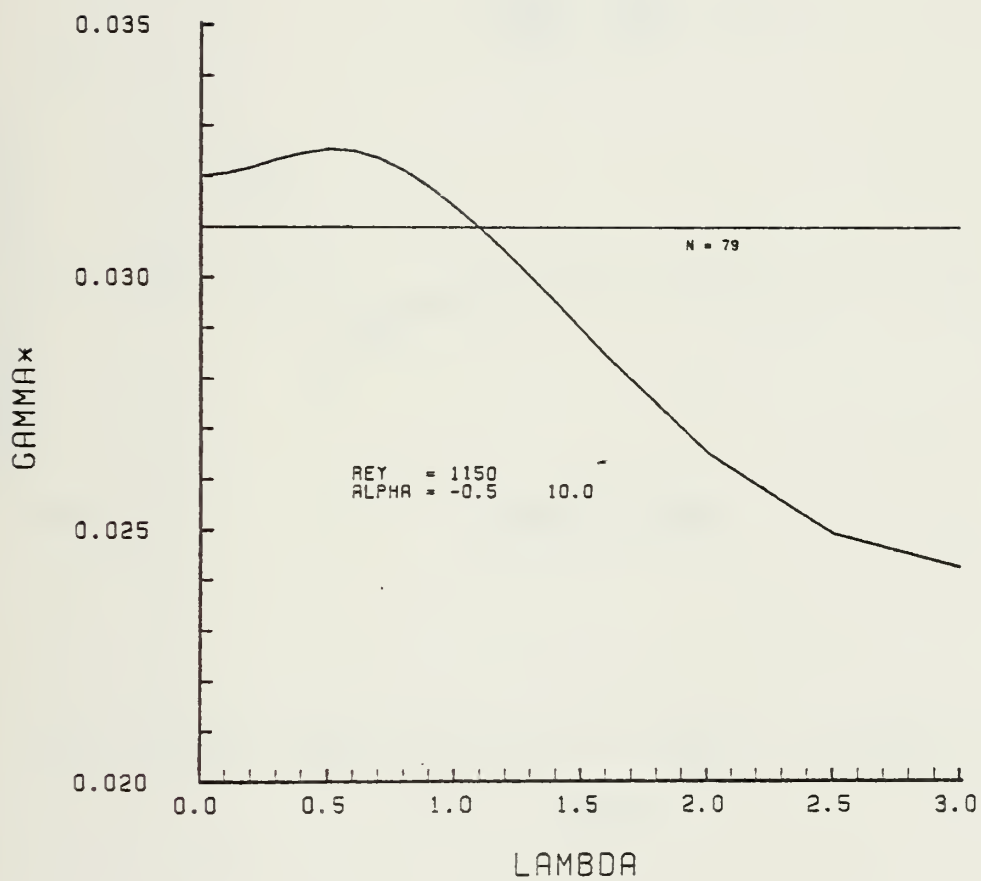


FIGURE 4-10. γ^* Versus Mesh Parameter, Lambda

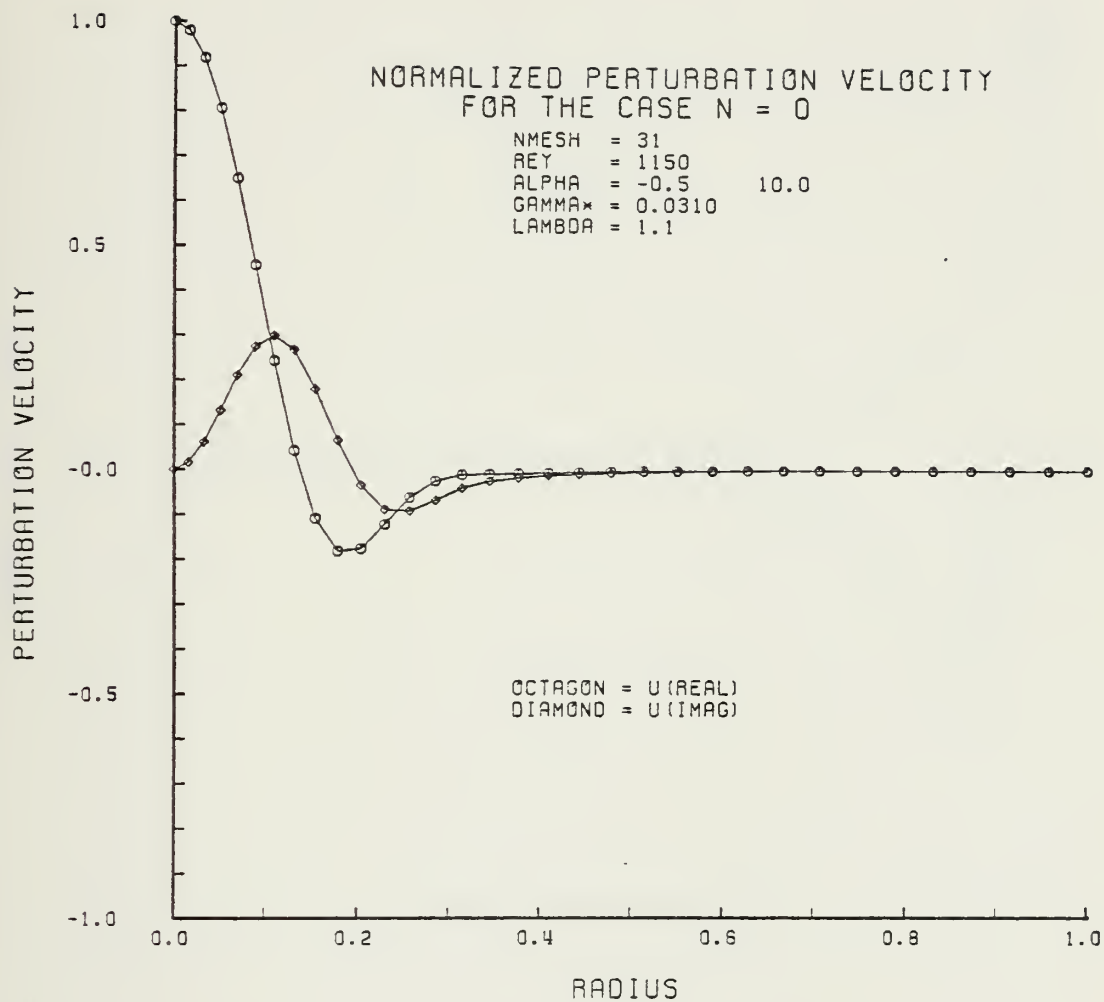


FIGURE 4-11

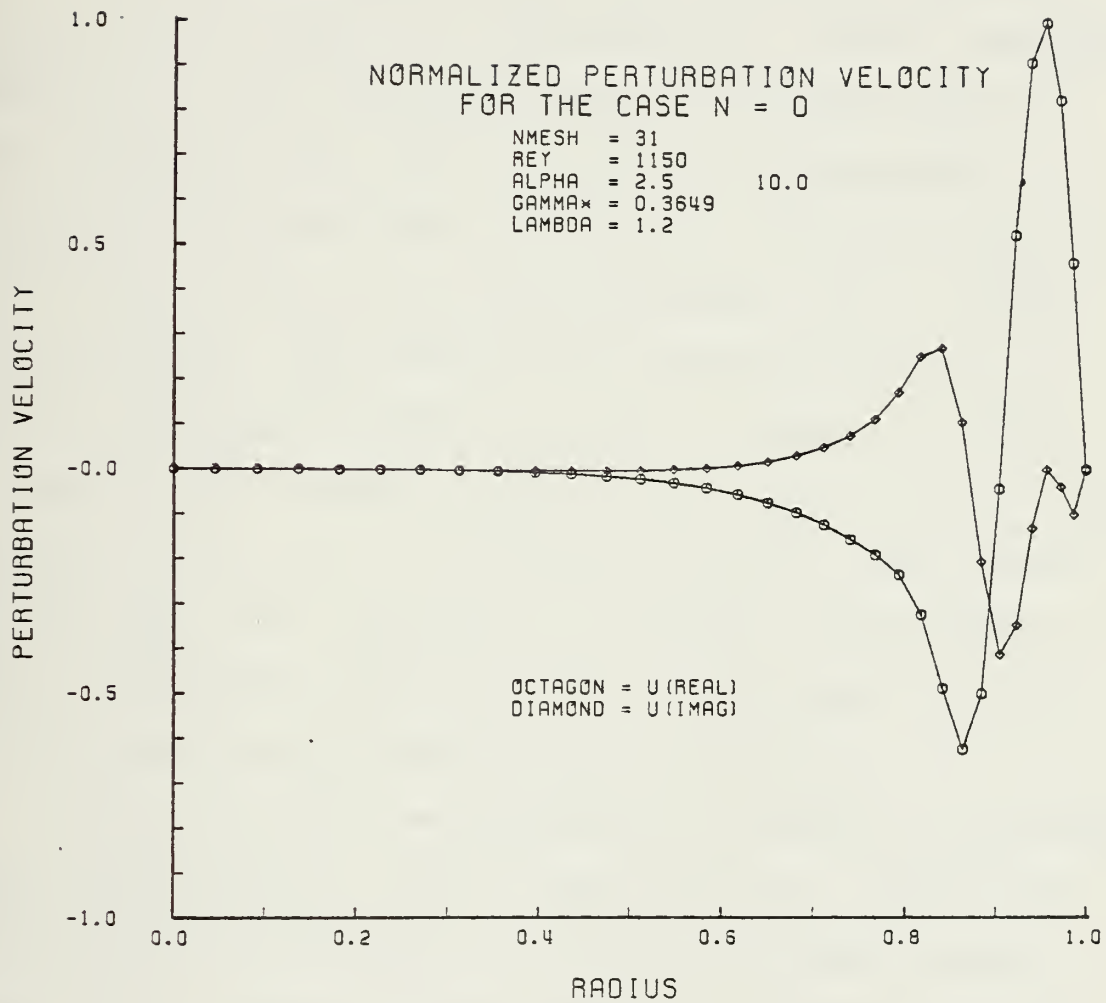


FIGURE 4-12

V. CONCLUSIONS AND RECOMMENDATIONS

The implementation of the newly developed boundary conditions of Gawain [9] has permitted a stable, numerical solution to the linearized vorticity transport equation. The results of the numerical solution are presented in Section IV and show that the stability of pipe Poiseuille flow is governed by the three parameters, α_R , α_I and R_e . In particular, both positive and negative values of α_R , that is, streamwise growth and decay in space, if sufficiently large, produce unstable growth rates in time. This result is new and it is consistent with the known experimental fact that transition to turbulent flow depends not only on Reynolds number but also on the general character of the perturbations which exist in the flow.

The perturbation velocity plots of Section IV represent the first practical look at the function Q . These plots were valuable indicators for adequacy of mesh fineness, that is, N , changes in the nature of the function Q and effects of a nonuniform mesh.

No instabilities were discovered for purely sinusoidal perturbations ($\alpha_R = 0$). This is consistent with the previous investigation of Ref. 11, but should not be assumed for investigations of other angular wave numbers, ($n = 1, 2, 3, \dots$).

Adequate numerical accuracy was proven by demonstrating that the solution was virtually independent of the number of mesh points, N , and that it satisfied to a high degree an independent check of the governing differential equation. This procedure should also be carried out in future investigations prior to conducting full scale data runs.

This study suggests that similar, and perhaps even more rewarding results will be obtained for the higher angular wave numbers. Although lengthy, programming is straightforward if approached systematically. The general organization of the programs of Ref. 4 or Ref. 6 should be helpful in this task. It is recommended that the case for $n = 1$ be undertaken as a follow-on to this study.

The nonuniform computational mesh was shown to be a powerful tool in the reduction of computational time. At the same time, however, the dependence of the mesh offset parameter, λ , on input conditions needs to be investigated further to realize the full potential of this technique.

APPENDIX A

DERIVATION OF VORTICITY TRANSPORT EQUATION COEFFICIENTS

From the change of variable introduced in Ref. 9, the function H for the case $n = 0$ is expressed by

$$H = rQ \quad (A-1)$$

Taking derivatives

$$DH = rDQ + Q \quad (A-2)$$

$$D^2H = rD^2Q + 2DQ \quad (A-3)$$

$$D^3H = rD^3Q + 3D^2Q \quad (A-4)$$

$$D^4H = rD^4Q + 4D^3Q \quad (A-5)$$

Let the '*' superscript denote element (2,2) of matrices (A1) through (A9) of Ref. 9. Since for $n = 0$, only the function H was investigated, equations (2-10) become

$$\begin{aligned} M_4^* D^4H + M_3^* D^3H + M_2^* D^2H + M_1^* DH + M_0^* H \\ - \gamma [N_2^* D^2H + N_1^* DH + N_0^* H] = 0 \end{aligned} \quad (A-6)$$

Substituting for H, equation (A-6) becomes

$$\begin{aligned}
& M_4^* \{rD^4Q + 4D^3Q\} + M_3^* \{rD^3Q + 3D^2Q\} + M_2^* \{rD^2Q + 2DQ\} \\
& + M_1^* \{rDQ + Q\} + M_0^* \{rQ\} - \gamma [N_2^* \{rD^2Q + 2DQ\} \\
& + N_1^* \{rDQ + Q\} + N_0^* \{rQ\}] = 0
\end{aligned} \tag{A-7}$$

Before proceeding further, it should be noted that the Ref. 9 matrices from which the coefficients for equation (A-7) were taken were obtained from matrices (2-10) through (2-17) of Ref. 6 by means of the following substitutions:

$$U = 2(1 - r^2) \tag{A-8}$$

$$t = \alpha^2 \frac{n_2}{r^2} \tag{A-9}$$

$$T = \alpha U - \frac{1}{R_e} \left(\alpha^2 - \frac{n_2}{r^2} \right) \tag{A-10}$$

Defining the new coefficients for equation (A-7) as M_0 through M_4 and N_0 through N_2

$$M_4 = rM_4^* = -\frac{r}{R_e} \tag{A-11}$$

$$M_3 = 4M_4^* + rM_3^* = -\frac{6}{R_e} \tag{A-12}$$

$$M_2 = 3M_3^* + rM_2^* = r\alpha U - \frac{1}{R_e} \left\{ \frac{3}{r} + 2\alpha^2 r \right\} \tag{A-13}$$

$$M_1 = 2M_2^* + rM_1^* = 3\alpha U + \frac{3}{R_e} \left\{ \frac{1}{r^2} - 2\alpha^2 \right\} \tag{A-14}$$

$$M_0 = M_1^* + rM_0^* = r\alpha^3 U - \frac{\alpha^4 r}{R_e} \tag{A-15}$$

$$N_2 = rN_2^* = -r \quad (\text{A-16})$$

$$N_1 = 2N_2^* + rN_1^* = -3 \quad (\text{A-17})$$

$$N_0 = N_1^* + rN_0^* = -\alpha^2 r \quad (\text{A-18})$$

Upon making use of the foregoing substitutions, the governing relation can finally be reduced to the form previously shown in equation (3-1).

APPENDIX B

FINITE DIFFERENCE EQUATIONS

Improved finite difference equations for the boundaries were obtained by not using the virtual point method of Ref. 4 and Ref. 6 and deriving the forms directly from the boundary conditions of Appendix A. The equations thus formed are also of consistent order truncation error, significantly improving the accuracy of the solution [Ref. 8].

Because of a peculiarity in the form of the consistent second order truncation error equations at the axis, a singularity resulted for α equal to zero. Consistent third order truncation error equations eliminated this problem.

From Appendix A, the axis boundary conditions are

$$DQ(0) = 0 \quad \text{and} \quad D^3Q(0) = 0 \quad (\text{B-1})$$

Representing Q by a power series and applying equations (B-1) yields

$$\begin{aligned} Q(r) = Q(0) + D^2Q(0)\frac{r^2}{2!} + D^4Q(0)\frac{r^4}{4!} + D^5Q(0)\frac{r^5}{5!} \\ + D^6Q(0)\frac{r^6}{6!} + \dots \end{aligned} \quad (\text{B-2})$$

Using five mesh points at $r = \delta, 2\delta, 3\delta, 4\delta$ and 5δ results in the matrix

$$\begin{bmatrix} Q_1 \\ Q_2 \\ Q_3 \\ Q_4 \\ Q_5 \end{bmatrix} = \begin{bmatrix} 1 & \frac{1}{2} & \frac{1}{24} & \frac{1}{120} & \frac{1}{720} \\ 1 & 2 & \frac{16}{24} & \frac{32}{120} & \frac{64}{720} \\ 1 & \frac{9}{2} & \frac{81}{24} & \frac{243}{120} & \frac{729}{720} \\ 1 & 8 & \frac{256}{24} & \frac{1024}{120} & \frac{4096}{720} \\ 1 & \frac{25}{2} & \frac{625}{24} & \frac{3125}{120} & \frac{15625}{720} \end{bmatrix} \begin{bmatrix} Q(0) \\ \delta^2 D^2 Q(0) \\ \delta^4 D^4 Q(0) \\ \delta^5 D^5 Q(0) \\ \delta^6 D^6 Q(0) \end{bmatrix} + O\delta^7$$

(B-3)

Differentiating equation (B-2) and substituting $r = \delta$ gives
(in matrix form)

$$\begin{bmatrix} Q(\delta) \\ \delta DQ(\delta) \\ \delta^2 D^2 Q(\delta) \\ \delta^3 D^3 Q(\delta) \\ \delta^4 D^4 Q(\delta) \end{bmatrix} = \begin{bmatrix} 1 & \frac{1}{2!} & \frac{1}{4!} & \frac{1}{5!} & \frac{1}{6!} \\ 0 & 1 & \frac{1}{3!} & \frac{1}{4!} & \frac{1}{5!} \\ 0 & 1 & \frac{1}{2!} & \frac{1}{3!} & \frac{1}{4!} \\ 0 & 0 & 1 & \frac{1}{2!} & \frac{1}{3!} \\ 0 & 0 & 1 & 1 & \frac{1}{2!} \end{bmatrix} \begin{bmatrix} Q(0) \\ \delta^2 D^2 Q(0) \\ \delta^4 D^4 Q(0) \\ \delta^5 D^5 Q(0) \\ \delta^6 D^6 Q(0) \end{bmatrix} + O\delta^7$$

(B-4)

Let [A] and [B] denote the coefficient matrices of equations (B-3) and (B-4) respectively. The values of $Q(0)$, $\delta^2 D^2 Q(0)$, $\delta^4 D^4 Q(0)$, $\delta^5 D^5 Q(0)$ and $\delta^6 D^6 Q(0)$ may be solved for by

$$\begin{bmatrix} Q(0) \\ \delta^2 D^2 Q(0) \\ \delta^4 D^4 Q(0) \\ \delta^5 D^5 Q(0) \\ \delta^6 D^6 Q(0) \end{bmatrix} = [A]^{-1} \begin{bmatrix} Q_1 \\ Q_2 \\ Q_3 \\ Q_4 \\ Q_5 \end{bmatrix} + O\delta^7 \quad (B-5)$$

Putting equation (B-5) into equation (B-4),

$$\begin{bmatrix} Q(\delta) \\ \delta DQ(\delta) \\ \delta^2 D^2 Q(\delta) \\ \delta^3 D^3 Q(\delta) \\ \delta^4 D^4 Q(\delta) \end{bmatrix} = [B][A]^{-1} \begin{bmatrix} Q_1 \\ Q_2 \\ Q_3 \\ Q_4 \\ Q_5 \end{bmatrix} + O\delta^7 \quad (B-6)$$

The last line of this set of equations gives

$$\begin{aligned} D^4 Q(\delta) &= \frac{1}{\delta^4} (-.911564626Q_1 + 2.750242955Q_2 - 3.043731779Q_3 \\ &\quad + 1.42468416Q_4 - .219630709Q_5) + O\delta^3 \end{aligned} \quad (B-7)$$

To solve for $D^3 Q(\delta)$, the rightmost column and bottom row are eliminated from matrices [A] and [B] then these new matrices are inserted into equations (B-5) and (B-6).

The bottom line of equation (B-6) will now give the expression for $D^3Q(\delta)$ with a consistent third order truncation error. $D^2Q(\delta)$ and $DQ(\delta)$ were solved for in a similar manner.

$$D^3Q(\delta) = \frac{1}{\delta^3}(1.825165563Q_1 - 3.250331126Q_2 + 1.660927152Q_3 - .235761589Q_4) + O\delta^3 \quad (B-8)$$

$$D^2Q = \frac{1}{\delta^2}(-\frac{35}{60}Q_1 + \frac{8}{15}Q_2 + \frac{1}{20}Q_3) + O\delta^3 \quad (B-9)$$

$$DQ = \frac{1}{\delta}(-\frac{2}{3}Q_1 + \frac{2}{3}Q_2) + O\delta^3 \quad (B-10)$$

Due to the complexity of the boundary conditions, it was decided that consistent third order truncation error equations should also be used at $r = 2\delta$. For this the [B] matrix only need be changed as equation (B-2) is unchanged at this station. The new matrix [B] is formed by differentiating equation (B-2) and making the substitution $r = 2\delta$. Proceeding as for $r = \delta$ gives the following finite difference approximations

$$D^4Q(2\delta) = \frac{1}{\delta^4}(-3.10340136Q_1 + 6.903012634Q_2 - 5.342274053Q_3 + 1.66083577Q_4 - 0.123420797Q_5) + O\delta^3 \quad (B-11)$$

$$D^3Q(2\delta) = \frac{1}{\delta^3}(.868874172Q_1 - .937748345Q_2 - .254304636Q_3 + .323178808Q_4) + O\delta^3 \quad (B-12)$$

$$D^2Q(2\delta) = \frac{1}{\delta^2} \left(\frac{11}{12}Q_1 - \frac{28}{15}Q_2 + \frac{19}{20}Q_3 \right) + O\delta^3 \quad (B-13)$$

$$DQ(2\delta) = \frac{1}{\delta} \left(-\frac{4}{3}Q_1 + \frac{4}{3}Q_2 \right) + O\delta^3 \quad (B-14)$$

It should also be noted that the value of Q at $r = 0$ may be solved for from the top line of equations (B-5)

$$Q(0) = (1.795918367Q_1 - 1.24781341Q_2 + .606413994Q_3 - .177842566Q_4 + .023323615Q_5) + O\delta^3 \quad (B-15)$$

The central difference equations given by Ref. 6 were already consistent second order truncation error equations as confirmed by Ref. 8 and were retained.

For the wall, the clamped end, consistent second order equations (5) through (8) of Table II, Ref. 8 were modified for the "right boundary" using the procedure given in Section 5 of that reference.

$$D^4Q(1-\delta) = \frac{1}{\delta^4} \left(-\frac{1}{4}Q_{N-3} + \frac{8}{3}Q_{N-2} - 9Q_{N-1} + 16Q_N \right) + O\delta^2 \quad (B-16)$$

$$D^3Q(1-\delta) = \frac{1}{\delta^3} \left(-\frac{1}{3}Q_{N-2} + 3Q_N \right) + O\delta^2 \quad (B-17)$$

$$D^2Q(1-\delta) = \frac{1}{\delta^2} (Q_{N-1} - 2Q_N) + O\delta^2 \quad (B-18)$$

$$DQ(1-\delta) = \frac{1}{\delta} \left(-\frac{1}{2}Q_{N-1} \right) + O\delta^2 \quad (B-19)$$

Since the wall finite difference approximations were of only second order truncation error, the approximations for DQ through D^4Q at $r = 1-2\delta$ were obtained directly from the central difference equations with $Q(1) = 0$.

$$D^4Q(1-2\delta) = \frac{1}{\delta^4}(Q_{N-3} - 4Q_{N-2} + 6Q_{N-1} - 4Q_N) + O\delta^2 \quad (B-20)$$

$$D^3Q(1-2\delta) = \frac{1}{\delta^3}(-\frac{1}{2}Q_{N-3} + Q_{N-2} - Q_N) + O\delta^2 \quad (B-21)$$

$$D^2Q(1-2\delta) = \frac{1}{\delta^2}(Q_{N-2} - 2Q_{N-1} + Q_N) + O\delta^2 \quad (B-22)$$

$$DQ(1-2\delta) = \frac{1}{\delta}(-\frac{1}{2}Q_{N-2} + \frac{1}{2}Q_N) + O\delta^2 \quad (B-23)$$

APPENDIX C

NONUNIFORM MESH

To control the distribution of a fixed number of mesh points, a change of the independent variable from r to η was performed.

$$Q = Q(\eta) \quad (C-1)$$

$$r = r(\eta) \quad (C-2)$$

The derivative with respect to r becomes

$$D = (D^* r)^{-1} D^* \quad (C-3)$$

where

$$D^* = \frac{d}{d\eta} \quad \text{and} \quad D = \frac{d}{dr} \quad (C-4)$$

$DQ, D^2Q \dots$ can now be expressed in terms of the new independent variable, η .

$$DQ = (D^* r)^{-1} D^* Q \quad (C-5)$$

$$\begin{aligned} D^2Q &= D(DQ) = (D^* r)^{-1} D^* (DQ) \\ &= (D^* r)^{-2} D^{*2} Q - (D^* r)^{-3} (D^{*2} r) D^* Q \end{aligned} \quad (C-6)$$

$$\begin{aligned}
D^3 Q &= D(D^2 Q) = (D^* R)^{-1} D^* (D^2 Q) \\
&= (D^* r)^{-3} D^{*3} Q - 3(D^* r)^{-4} (D^{*2} r) D^{*2} Q \\
&\quad - [(D^* r)^{-4} (D^{*3} r) - 3(D^* r)^{-5} (D^{*2} r)^2] DQ \quad (C-7)
\end{aligned}$$

$$\begin{aligned}
D^4 Q &= D(D^3 Q) = (D^* r)^{-1} D^* (D^3 Q) \\
&= (D^* r)^{-4} D^{*4} Q - 6(D^* r)^{-5} (D^{*2} r) D^{*3} Q \\
&\quad + [15(D^* r)^{-6} (D^{*2} r) - 4(D^* r)^{-5} (D^{*3} r)] D^{*2} Q \\
&\quad - [15(D^* r)^{-7} (D^{*2} r)^3 - 10(D^* r)^{-6} (D^{*2} r) (D^{*3} r) \\
&\quad + (D^* r)^{-5} (D^{*4} r)] DQ \quad (C-8)
\end{aligned}$$

The derivatives of Q with respect to r can now be written

$$DQ = f_{11} D^* Q \quad (C-9)$$

$$D^2 Q = f_{22} D^{*2} Q + f_{21} D^* Q \quad (C-10)$$

$$D^3 Q = f_{33} D^{*3} Q + f_{32} D^{*2} Q + f_{31} D^* Q \quad (C-11)$$

$$D^4 Q = f_{44} D^{*4} Q + f_{43} D^{*3} Q + f_{42} D^{*2} Q + f_{41} D^* Q \quad (C-12)$$

where

$$f_{11} = (D^* r)^{-1} \quad (C-13)$$

$$f_{22} = (D^* r)^{-2} \quad (C-14)$$

$$f_{21} = -(D^* r)^{-3} (D^{*2} r) \quad (C-15)$$

$$f_{33} = (D^* r)^{-3} \quad (C-16)$$

$$f_{32} = -3 (D^* r)^{-4} (D^{*2} r) \quad (C-17)$$

$$f_{31} = 3 (D^* r)^{-5} (D^{*2} r)^2 - (D^* r)^{-4} (D^{*3} r) \quad (C-18)$$

$$f_{44} = (D^* r)^{-4} \quad (C-19)$$

$$f_{43} = -6 (D^* r)^{-5} (D^{*2} r) \quad (C-20)$$

$$f_{42} = 15 (D^* r)^{-6} (D^{*2} r)^2 - 4 (D^* r)^{-5} (D^{*3} r) \quad (C-21)$$

$$f_{41} = -15 (D^* r)^{-7} (D^{*2} r)^3 + 10 (D^* r)^{-6} (D^{*2} r) (D^{*3} r) \\ - (D^* r)^{-5} (D^{*4} r) \quad (C-22)$$

Substituting equations (C-9) through (C-12) into the vorticity transport equation (A-6) yields

$$M_4^* D^{*4} Q + M_3^* D^{*3} Q + M_2^* D^{*2} Q + M_1^* D^* Q + M_0^* Q \\ - \gamma [N_2^* D^{*2} Q + N_1^* D^* Q + N_0^* Q] = 0 \quad (C-23)$$

where

$$M_4^* = M_4 f_{44} \quad (C-24)$$

$$M_3^* = M_4 f_{43} + M_3 f_{33} \quad (C-25)$$

$$M_2^* = M_4 f_{42} + M_3 f_{32} + M_2 f_{22} \quad (C-26)$$

$$M_1^* = M_4 f_{41} + M_3 f_{31} + M_2 f_{21} \quad (C-27)$$

$$M_0^* = M_0 \quad (C-28)$$

$$N_2^* = N_2 f_{22} \quad (C-29)$$

$$N_1^* = N_2 f_{21} + N_1 f_{11} \quad (C-30)$$

$$N_0^* = N \quad (C-31)$$

In order to concentrate the mesh points at the axis, the function

$$r = 1 - C \tanh \lambda(1-\eta) \quad (C-32)$$

was chosen where λ is a parameter controlling the degree of concentration of mesh points near the axis. Equation (C-32) must satisfy the two conditions

$$r = 0 \quad \text{at} \quad \eta = 0 \quad (C-33)$$

and

$$r = 1 \quad \text{at} \quad \eta = 1 .$$

Substituting equation (C-33) into (C-32) gives

$$C = 1/\tanh \lambda . \quad (C-35)$$

Computing derivatives

$$D^* r = C\lambda / \cosh^2 \lambda (1-\eta) \quad (C-36)$$

$$D^{*2} r = 2C\lambda^2 [\tanh \lambda (1-\eta) / \cosh^2 \lambda (1-\eta)] \quad (C-37)$$

$$D^{*3} r = -2C\lambda^3 \{ [1-2\sinh^2 \lambda (1-\eta)] / \cosh^4 \lambda (1-\eta) \} \quad (C-38)$$

$$D^{*4} r = 8C\lambda^4 [\tanh^3 \lambda (1-\eta) / \cosh^2 \lambda (1-\eta)] \quad (C-39)$$

To shift the mesh point concentration to the wall, the function

$$r = C \tanh \lambda \eta \quad (C-40)$$

was selected. Satisfying equations (C-33) and (C-34) for this equation also gives equation (C-35). The derivatives

of (C-40) are given by equations (C-36) through (C-39) if η is substituted for all occurrences of $(1-\eta)$ and the signs of equations (C-37) and (C-39) are reversed. Figures C-1 and C-2 show equations (C-32) and (C-40) for four selected values of the parameter λ .

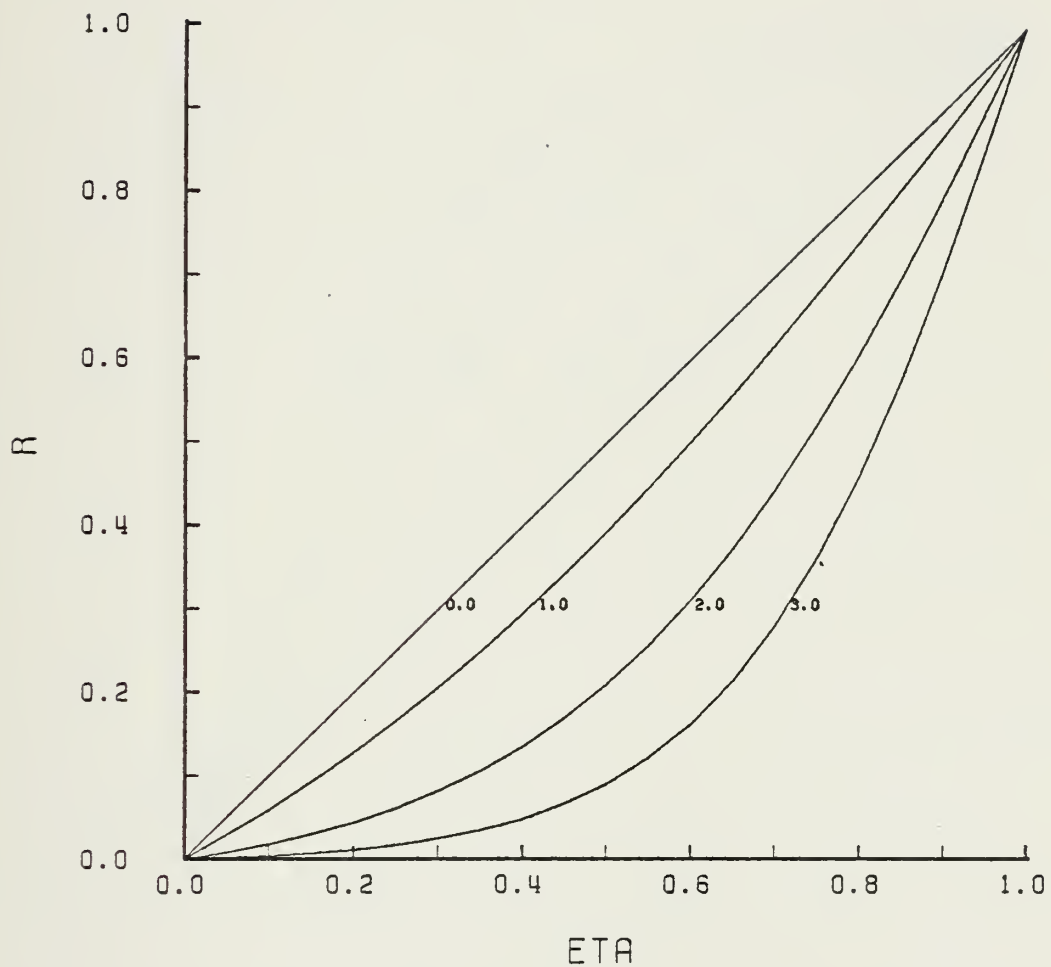


FIGURE C-1. R Versus η for Four Selected Values of λ - Axis Offset

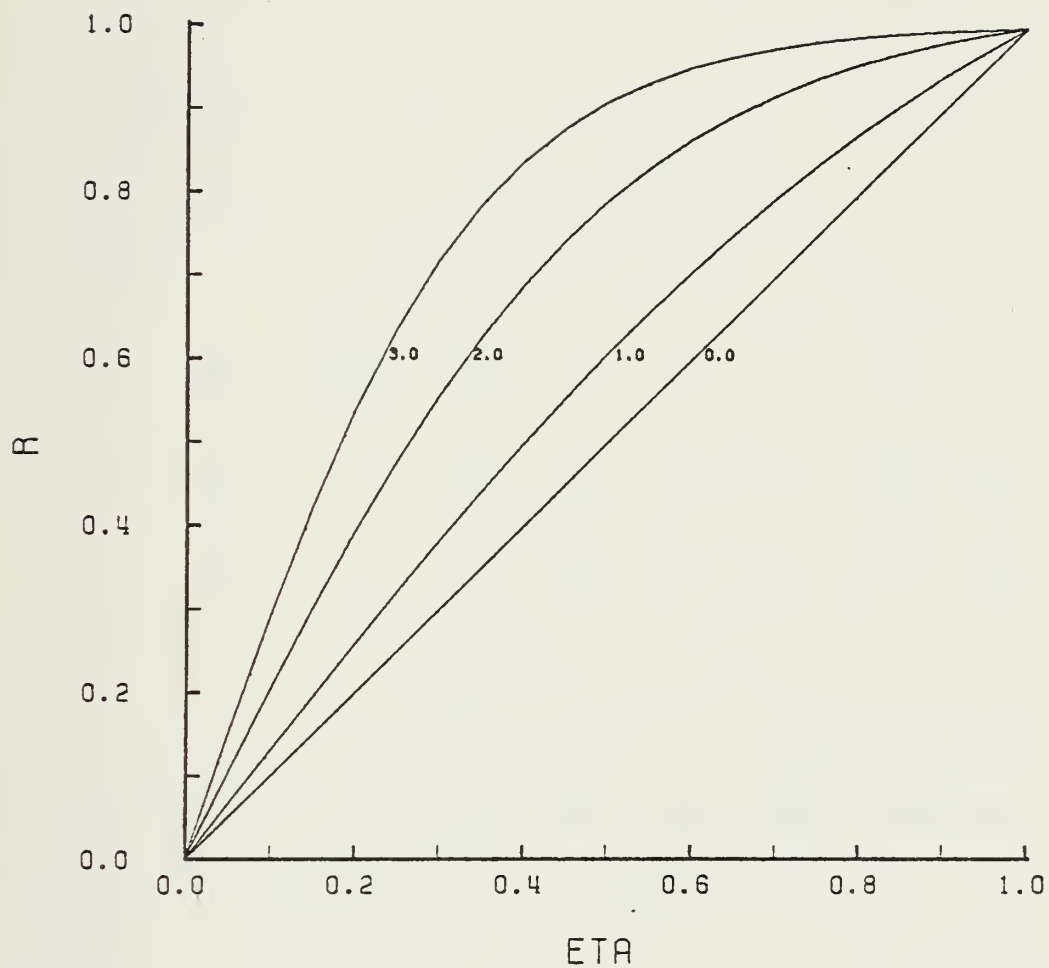


FIGURE C-2. R Versus η for Four Selected Values of λ - Wall Offset

APPENDIX D

DERIVATION OF PERTURBATION VELOCITIES

From Ref. 4, Appendix E, equations E-6 through E-8:

$$\begin{Bmatrix} u(r) \\ v(r) \\ w(r) \end{Bmatrix} = [A]\bar{W} + [B]D\bar{W} \quad (D-1)$$

$$= \begin{bmatrix} 0 & -\frac{\beta}{r} & \frac{1}{r} \\ \frac{\beta}{r} & 0 & -\alpha \\ 0 & \alpha & 0 \end{bmatrix} \begin{Bmatrix} F \\ G \\ H \end{Bmatrix} + \begin{bmatrix} 0 & 0 & 1 \\ 0 & 0 & 0 \\ -1 & 0 & 0 \end{bmatrix} \begin{Bmatrix} DF \\ DG \\ DG \end{Bmatrix} \quad (D-2)$$

For this case $\beta = \eta_i = 0$ and $F = DF = 0$. Restricting the investigation to the function H for the reason expressed in Section I and solving for $u(r)$ gives

$$u(r) = \frac{H}{r} + DH \quad (D-3)$$

Performing the change of variable

$$H = rQ \quad (D-4)$$

$$DH = Q + rDQ \quad (D-5)$$

$$u(r) = \frac{rQ}{r} + (Q + rDQ) = 2Q + rDQ \quad (D-6)$$

In order to implement this derivation in a numerical analysis, equation (D-6) was rewritten as

$$u_i = 2Q_i + r_i DQ_i \quad (D-7)$$

Performing the change of independent variable (Appendix C) to accommodate a nonuniform mesh

$$Q_i = Q(\eta_i) \quad (D-8)$$

$$r_i = r(\eta_i) \quad (D-9)$$

$$DQ_i = (D^* r_i)^{-1} D^* Q(\eta_i) \quad (D-10)$$

Substituting equations (D-8), (D-9) and (D-10) into equation (D-7) gives

$$u_i = 2Q(\eta_i) + r(\eta_i) D^* r_i^{-1} D^* Q(\eta_i) \quad (D-11)$$

For the axis offset nonuniform mesh, $r(\eta)$ is given by equation (C-32) and $(D^* r)$ by equation (C-36). Substituting into equation (D-11) using equation (C-35) results in

$$\begin{aligned}
u_i &= 2Q(\eta_i) + \left\{ 1 - \frac{\tanh[\lambda(1-\eta_i)]}{\tanh \lambda} \right\} \left\{ \frac{\cosh^2[\lambda(1-\eta_i)]}{C\lambda} \right\} D^* Q(\eta_i) \\
&= 2Q(\eta_i) + \left\{ 1 - \frac{\tanh[\lambda(1-\eta_i)]}{\tanh \lambda} \right\} \frac{\tanh \lambda \cosh^2[\lambda(1-\eta_i)]}{\lambda} \left\{ D^* Q(\eta_i) \right\}
\end{aligned}
\tag{D-12}$$

For the wall offset mesh, equation (C-40) is substituted for equation (C-32) and all occurrences of the term $1-\eta_i$ are replaced by the term η_i .

The value of u at the axis (u_0) and at the wall (u_{N+1}) were solved for by using the boundary conditions specified in Ref. 9, namely

$$Q(1) = 0 \tag{D-13}$$

$$DQ(1) = 0 \tag{D-14}$$

$$DQ(0) = 0 \tag{D-15}$$

$$D^3Q(0) = 0 \tag{D-16}$$

From equations (D-13) and (D-14), using equation (D-7) it is obvious that

$$u_{N+1} = 0 \tag{D-17}$$

and from equations (D-15) and (D-7), it is similarly found that

$$u_0 = 2Q(0) ,$$

(D-18)

where the finite difference approximation for $Q(0)$ is given by equation (B-15).

[illegible]


```

C      IF MODENO = 3, THIS OUTPUT IS INHIBITED.  MODENO MUST BE
C      SET EQUAL TO ONE TO GENERATE CORRECT DATA FOR PROGRAM EIGFCN.
C      *****
C      1 WRITE (6,9) AMDA
C        READ (5,11) AMDA
C        KSET = 0
C        IF (AMDA.LT.-1.D-10) KSET=-1
C        IF (AMDA.GT.1.D-10) KSET=1
C        WRITE (6,10)
C        READ (5,11) AR
C        WRITE (6,12) AI
C        READ (5,11) AI
C        WRITE (6,13) REY
C        READ (5,11) REY
C        IF (REY.LE.0.D0) GO TO 5
C        CALL STAB (AR, AI, GRMAX, KSET, MODENO)
C        WRITE (6,14) GRMAX
C        GO TO 1
C      *****
C      COMPUTE STABILITY MAP (MODENO = 2)
C
C      COMPUTES A STABILITY MAP AT MESH POINTS ESTABLISHED BY
C      THE FOLLOWING PARAMETERS READ FROM FILE FTO1FOO1:
C
C      NXSTP - NO OF MESH PTS IN X-DIRECTION
C      NYSTP - NO OF MESH PTS IN Y-DIRECTION
C      N - DIMENSION OF MATRICES X & Y IN SUBROUTINE STAB
C      DELAR - MAGNITUDE OF THE X-DIRECTION STEP
C      DELAI - MAGNITUDE OF THE Y-DIRECTION STEP
C      REY - REYNOLDS NUMBER
C
C      **NOTE - RUN TIME IS LONG IN THIS MODE, SO CP/CMS
C      RUNS SHOULD BE LIMITED TO 10X10 MESHES, OR LESS WITH
C      N = 31. LARGER RUNS SHOULD BE MADE UNDER BATCH.
C      LITTLE OS MAY ALSO BE USED AS LESS THAN 18CK OF
C      CORE IS REQUIRED IN THIS MODE FOR N <= 47.
C
C      **NOTE - TO RUN THE MAPPING PORTION UNDER OS OR LITTLE OS,
C      PERFORM THE FOLLOWING:
C
C      1) RETAIN ALL MAIN PROGRAM SECTIONS BRACKETED BY '-----'.
C      2) CHANGE ALL READ DEVICES TO '5'. VICE '1' IN MAIN PROGRAM.
C      3) CHANGE THE DEVICE CODE OF THE LAST WRITE STATEMENT

```


[illegible]

C	DO 2 I=1,MDIM	STAB1250
	RADIUS(I) = DFLOAT(I)*DELL0	STAB1260
	WRITE (2,7) RADIUS(I),ZR(I,NEIG),ZI(I,NEIG)	STAB1270
C	-----	STAB1280
	2 CONTINUE	STAB1290
C	3 RETURN	STAB1300
C	4 FCRMAT ('0* * * ERROR NUMBER',I7,' ON EIGENVALUE',	STAB1310
	17,' * * *',//)	STAB1320
	5 FORMAT (I2,3D20.10)	STAB1330
	6 FCRMAT (I2)	STAB1340
	7 FCRMAT (F15.7,2(1PD20.10))	STAB1350
	END	STAB1360
		STAB1370
		STAB1380
		STAB1390
CSUBROUTINE MSET1(ETA,CQM1,CQM2,KSET).....	MST110
C	PURPOSE	MST120
C	MSET1 GENERATES THE COEFFICIENTS FOR THE FINITE DIFFERENCE	MST130
C	APPROXIMATION OF THE COMPONENT Q.	MST140
C	USAGE	MST150
C	CALL MSET1(ETA,CQM1,CQM2,KSET)	MST160
C	DESCRIPTION OF PARAMETERS	MST170
C	ETA - INDEPENDENT VARIABLE REPLACING R	MST180
C	IN NONUNIFORM MESH.	MST190
C	CQM1 - COEFFICIENTS OF Q AND ITS DERIVATIVES	MST200
C	IN THE FINITE DIFFERENCE APPROXIMATION OF	MST210
C	THE NON-GAMMA TERMS. CQM1(1) IS THE	MST220
C	COEFFICIENT FOR Q, CQM1(2) IS THE COEF-	MST230
C	FICIENT FOR DQ, AND SO ON TO CQM1(5).	MST240
C	CQM2 - SAME AS CQM1 EXCEPT GAMMA TERMS AND	MST250
C	DIMENSIONED 3 INSTEAD OF 5.	MST260
C	KSET - MESH OFFSET PARAMETER AS DESCRIBED FOR	MST270
C	SUBROUTINE STAB.	MST280
C	OTHER ROUTINES NEEDED	MST290
C	NONE	MST300
		MST310

[illegible]


```
1 X(I,J) = (ODO,ODO)
```

C
C
C
C
C
C

```
ESTABLISH THE CENTRAL DIFFERENCE APPROXIMATION AT EACH POINT IN  
THE MESH.
```

```
ETA = DEL  
CALL MSET1 (ETA, CQM1, CQM2, KSET)  
X(1,1) = CFMAT(1,1,CQM1,CQM2)  
X(1,2) = CFMAT(1,2,CQM1,CQM2)  
X(1,3) = CFMAT(1,3,CQM1,CQM2)  
X(1,4) = CFMAT(1,4,CQM1,CQM2)  
X(1,5) = CFMAT(1,5,CQM1,CQM2)
```

C

```
ETA = 2DO*DEL  
CALL MSET1 (ETA, CQM1, CQM2, KSET)  
X(2,1) = CFMAT(2,1,CQM1,CQM2)  
X(2,2) = CFMAT(2,2,CQM1,CQM2)  
X(2,3) = CFMAT(2,3,CQM1,CQM2)  
X(2,4) = CFMAT(2,4,CQM1,CQM2)  
X(2,5) = CFMAT(2,5,CQM1,CQM2)
```

C
C

```
IL = N-2
```

```
DO 2 I=3,IL
```

```
K=1-3
```

```
ETA = DEL*DFLOAT(I)
```

```
CALL MSET1 (ETA, CQM1, CQM2, KSET)
```

C

```
DO 2 J=1,5
```

```
2 X(I,K+J) = CFMAT(3,J,CQM1,CQM2)
```

C
C

```
ETA = 1DO-2 DO*DEL  
CALL MSET1 (ETA, CQM1, CQM2, KSET)  
X(N-1,N-3) = CFMAT(4,1,CQM1,CQM2)  
X(N-1,N-2) = CFMAT(4,2,CQM1,CQM2)  
X(N-1,N-1) = CFMAT(4,3,CQM1,CQM2)  
X(N-1,N) = CFMAT(4,4,CQM1,CQM2)
```

C

```
ETA = 1DO-DEL  
CALL MSET1 (ETA, CQM1, CQM2, KSET)  
X(N,N-3) = CFMAT(5,1,CQM1,CQM2)  
X(N,N-2) = CFMAT(5,2,CQM1,CQM2)  
X(N,N-1) = CFMAT(5,3,CQM1,CQM2)  
X(N,N) = CFMAT(5,4,CQM1,CQM2)
```

MST12 580
MST12 590
MST12 600
MST12 610
MST12 620
MST12 630
MST12 640
MST12 650
MST12 660
MST12 670
MST12 680
MST12 690
MST12 700
MST12 710
MST12 720
MST12 730
MST12 740
MST12 750
MST12 760
MST12 770
MST12 780
MST12 790
MST12 800
MST12 810
MST12 820
MST12 830
MST12 840
MST12 850
MST12 860
MST12 870
MST12 880
MST12 890
MST12 900
MST12 910
MST12 920
MST12 930
MST12 940
MST12 950
MST12 960
MST12 970
MST12 980
MST12 990
MST12 1000
MST12 1010
MST12 1020
MST12 1030
MST12 1040
MST12 1050

RETURN
END

MSI21060
MSI21070

.....FUNCTION CQM1E1(JSTA,K,CQM1,CQM2).....
(POLAR COORDINATES)

CQM1 10
CQM1 20
CQM1 30
CQM1 40
CQM1 50
CQM1 60
CQM1 70
CQM1 80
CQM1 90
CQM1 100
CQM1 110
CQM1 120
CQM1 130
CQM1 140
CQM1 150
CQM1 160
CQM1 170
CQM1 180
CQM1 190
CQM1 200
CQM1 210
CQM1 220
CQM1 230
CQM1 240
CQM1 250
CQM1 260
CQM1 270
CQM1 280
CQM1 290
CQM1 300
CQM1 310
CQM1 320
CQM1 330
CQM1 340
CQM1 350
CQM1 360
CQM1 370
CQM1 380
CQM1 390
CQM1 400
CQM1 410
CQM1 420
CQM1 430
CQM1 440

PURPOSE

RETURNS THE VALUES FOR THE COEFFICIENTS IN THE ARRAYS
REPRESENTING THE CENTRAL DIFFERENCE APPROXIMATION OF THE
VORTICITY TRANSPORT EQUATION USING THE COEFFICIENTS COMPUTED
BY SUBROUTINE MSET1.

DESCRIPTION OF PARAMETERS

JSTA - INDICATES WHICH DIFFERENCE EQUATION SET WILL BE USED.

- JSTA=1 - CONSISTENT 3RD ORDER TRUNCATION ERROR FINITE
DIFFERENCE EQUATIONS FOR R=DEL WILL BE USED.
- JSTA=2 - SAME AS ABOVE BUT R=2D0*DEL
- JSTA=3 - CENTRAL DIFFERENCE EQUATIONS WITH CONSISTENT 2ND
ORDER TRUNCATION ERROR WILL BE USED.
- JSTA=4 - SAME AS JSTA=3 BUT FOR R=1C0-2D0*DEL.
- JSTA=5 - SAME AS ABOVE BUT FOR R=1D0-DEL.

K - INDICATES THE ABSOLUTE POSITION OF THE POINT IN EACH ROW
OF THE FINITE DIFFERENCE MESH. IF THE FIRST NON-ZERO ENTRY
IN ROW J IS ELEMENT(J,3), THEN K=1 DENOTES ELEMENT(J,3),
K=2 DENOTES ELEMENT(J,4), ETC.

CQM1,CQM2 - THE COEFFICIENT ARRAYS FOR THE FINITE DIFFERENCE
APPROXIMATION OF THE FUNCTION Q. CQM1 CONTAINS THE
COEFFICIENTS FOR THE NON-GAMMA TERMS, WHILE CQM2 CONTAINS
THE COEFFICIENTS OF THE GAMMA TERMS. BOTH ARRAYS MUST BE
DIMENSIONED COMPLEX*16.

EXAMPLE OF THE CALLING ARGUMENT:

CQ M(1,2) E1(JSTA,K,CQM1,CQM2)

CQ - Q COMPONENT OF THE VELOCITY VECTOR POTENTIAL.

M(1,2) - 1 REFERS TO TERMS NOT CONTAINING GAMMA AS A
FACTOR.

2 REFERS TO TERMS CONTAINING GAMMA AS A FACTOR.


```

123D0*CQM1(3)/(15D0*DEL**2)+4D0*CQM1(2)/(3D0*DEL)+CQM1(1)
GO TO 29
10 CQM1E1 = -5.342274053D0*CQM1(5)/DEL**4-.254304636D0*CQM1(4)/DEL**3
1+19D0*CQM1(3)/(20D0*DEL**2)
GO TO 29
11 CQM1E1 = 1.666083577D0*CQM1(5)/DEL**4+.3251788C8D0*CQM1(4)/DEL**3
GO TO 29
12 CQM1E1 = -0.123420797D0*CQM1(5)/DEL**4
GO TO 29

```

C
C
C

CENTRAL DIFFERENCE APPROXIMATION FOR COMPONENT Q (NON GAMMA).

```

13 GO TO (14,15,16,17,18), K
14 CQM1E1 = CQM1(5)/DEL**4-CQM1(4)/(2D0*DEL**3)
GO TO 29
15 CQM1E1 = -4D0*CQM1(5)/DEL**4+CQM1(4)/DEL**3+CQM1(3)/DEL**2-CQM1(2)
1/(2D0*DEL)
GO TO 29
16 CQM1E1 = 6D0*CQM1(5)/DEL**4-2D0*CQM1(3)/DEL**2+CQM1(1)
GO TO 29
17 CQM1E1 = -4D0*CQM1(5)/DEL**4-CQM1(4)/DEL**3+CQM1(3)/DEL**2+CQM1(2)
1/(2D0*DEL)
GO TO 29
18 CQM1E1 = CQM1(5)/DEL**4+CQM1(4)/(2D0*DEL**3)
GO TO 29

```

C
C
C

FINITE DIFFERENCE EQUATIONS AT ETA=1D0-2D0*DEL (NCN-GAMMA).

```

19 GO TO (20,21,22,23), K
20 CQM1E1 = CQM1(5)/DEL**4-0.5D0*CQM1(4)/DEL**3
GO TO 29
21 CQM1E1 = -4D0*CQM1(5)/DEL**4+CQM1(4)/DEL**3+CQM1(3)/DEL**2-CQM1(2)
1/(2D0*DEL)
GO TO 29
22 CQM1E1 = 6D0*CQM1(5)/DEL**4-2D0*CQM1(3)/DEL**2+CQM1(1)
GO TO 29
23 CQM1E1 = -4D0*CQM1(5)/DEL**4-CQM1(4)/DEL**3+CQM1(3)/DEL**2+CQM1(2)
1/(2D0*DEL)
GO TO 29

```

C
C
C

FINITE DIFFERENCE EQUATIONS AT ETA=1D0-DEL (NON GAMMA).

```

24 GO TO (25,26,27,28), K
25 CQM1E1 = -0.25D0*CQM1(5)/DEL**4
GO TO 29
26 CQM1E1 = 8D0*CQM1(5)/(3D0*DEL**4)-CQM1(4)/(3D0*DEL**3)
GO TO 29
27 CQM1E1 = -9D0*CQM1(5)/DEL**4+CQM1(3)/DEL**2-CQM1(2)/(2D0*DEL)
GO TO 29

```



```

GO TO 29
28 CQM1E1 = 16D0*CQM1(5)/DEL**4+3D0*CQM1(4)/DEL**3-2D0*CQM1(3)/DEL**2
1+CQM1(1)
25 RETURN
C
ENTRY CQM2E1(JSTA,K,CQM1,CQM2)
C
GO TO (30,35,40,45,5C), JSTA
C
FINITE DIFFERENCE EQUATIONS AT ETA=DEL ( GAMMA ).
C
30 GO TO (31,32,33,34,34), K
31 CQM2E1 = -35D0*CQM2(3)/(60D0*DEL**2)-2D0*CQM2(2)/(3D0*DEL)+CQM2(1)
GO TO 54
32 CQM2E1 = 8D0*CQM2(3)/(15D0*DEL**2)+2D0*CQM2(2)/(3D0*DEL)
GO TO 54
33 CQM2E1 = CQM2(3)/(20D0*DEL**2)
GO TO 54
34 CQM2E1 = (0D0,0D0)
GO TO 54
C
FINITE DIFFERENCE EQUATIONS AT ETA=2D0*DEL ( GAMMA )
C
35 GO TO (36,37,38,39,35), K
36 CQM2E1 = 11D0*CQM2(3)/(12D0*DEL**2)-4D0*CQM2(2)/(3D0*DEL)
GO TO 54
37 CQM2E1 = -28D0*CQM2(3)/(15D0*DEL**2)+4D0*CQM2(2)/(3D0*DEL)+CQM2(1)
GO TO 54
38 CQM2E1 = 19D0*CQM2(3)/(20D0*DEL**2)
GO TO 54
39 CQM2E1 = (0D0,0D0)
GO TO 54
C
CENTRAL DIFFERENCE EQUATIONS FOR THE COMPONENT Q ( GAMMA ).
C
40 GO TO (41,42,43,44,41), K
41 CQM2E1 = (0D0,0D0)
GO TO 54
42 CQM2E1 = CQM2(3)/DEL**2-CQM2(2)/(2D0*DEL)
GO TO 54
43 CQM2E1 = -2D0*CQM2(3)/DEL**2+CQM2(1)
GO TO 54
44 CQM2E1 = CQM2(3)/DEL**2+CQM2(2)/(2D0*DEL)
GO TO 54
C
FINITE DIFFERENCE EQUATIONS AT ETA=1D0-2D0*DEL ( GAMMA ).
C
45 GC TO (49,46,47,48), K
46 CQM2E1 = CQM2(3)/DEL**2-CQM2(2)/(2D0*DEL)

```



```

47      GC TO 54
      CQM2E1 = -2D0*CQM2(3)/DEL**2+CQM2(1)
      GC TO 54
48      CQM2E1 = CQM2(3)/DEL**2+CQM2(2)/(2D0*DEL)
      GO TO 54
49      CQM2E1 = (OD0,OD0)
      GC TO 54

      FINITE DIFFERENCE EQUATIONS AT ETA=1D0-DEL ( GAMMA ).

50      GO TO (53,52,51,52), K
51      CQM2E1 = CQM2(3)/DEL**2-CQM2(2)/(2D0*DEL)
      GO TO 54
52      CQM2E1 = -2D0*CQM2(3)/DEL**2+CQM2(1)
      GO TO 54
53      CQM2E1 = (OD0,OD0)
54      RETURN
      END

```

۷۷۷

.....	SUBROUTINE CDMTIN(N,A,NDIM,IERR).....	0
PURPOSE		1
INVERT A COMPLEX*16 MATRIX		2
USAGE		3
CALL CDMTIN(N,A,NDIM,DETERM)		4
DESCRIPTION OF PARAMETERS		5
N	- ORDER OF COMPLEX*16 MATRIX TO BE INVERTED (INTEGER) MAXIMUM 'N' IS 100	6
A	- COMPLEX*16 INPUT MATRIX (DESTROYED). THE INVERSE OF 'A' IS RETURNED IN ITS PLACE	7
NDIM	- THE SIZE TO WHICH 'A' IS DIMENSIONED (ROW DIMENSION OF 'A' ACTUALLY APPEARING IN THE DIMENSION STATEMENT OF USER'S CALLING PROGRAM)	8
IERR	- ERROR PARAMETER RETURNED BY CDMTIN. IERR = 0 INDICATES NORMAL INVERSION. IERR = 9999 INDICATES SINGULAR MATRIX.	9
REMARKS		10


```

C      MATRIX 'A' MUST BE A COMPLEX*16 GENERAL MATRIX          CDMT 290
C      IF MATRIX 'A' IS SINGULAR THAT MESSAGE IS PRINTED      CDMT 300
C      'N' MUST BE .LE. NDIM                                   CDMT 310
C                                                                CDMT 320
C      SLBRoutines AND FUNCTIONS REQUIRED                         CDMT 330
C      ONLY BUILT-IN FORTRAN FUNCTIONS                         CDMT 340
C                                                                CDMT 350
C      METHOD                                                    CDMT 360
C                                                                CDMT 370
C      GAUSSIAN ELIMINATION WITH COLUMN PIVOTING IS USED.      CDMT 380
C                                                                CDMT 390
C      .....                                                    CDMT 400
C                                                                CDMT 410
C      SUBROUTINE CDMT IN (N,A,NDIM, IERR)                      CDMT 420
C      IMPLICIT REAL*8(A-H,O-Z)                                CDMT 430
C      INTEGER *4 IPIVOT(100), INDEX(100,2), IERR              CDMT 440
C      REAL *8 TEMP, ALPHA(100)                                CDMT 450
C      COMPLEX *16 A(NDIM,NDIM), PIVOT(100), AMAX,T,SWAP,U      CDMT 460
C                                                                CDMT 470
C      INITIALIZATION                                           CDMT 480
C                                                                CDMT 490
C      DO 2 J=1,N                                               CDMT 500
C      IERR = 0                                                 CDMT 510
C      ALPHA(J) = 0DO                                           CDMT 520
C                                                                CDMT 530
C      DO 1 I=1,N                                               CDMT 540
C      1 ALPHA(J) = ALPHA(J)+A(J,I)*DCONJG(A(J,I))              CDMT 550
C                                                                CDMT 560
C      2 ALPHA(J) = DSQRT(ALPHA(J))                             CDMT 570
C      2 IPIVOT(J) = 0                                           CDMT 580
C                                                                CDMT 590
C                                                                CDMT 600
C                                                                CDMT 610
C      DO 16 I=1,N                                              CDMT 620
C      SEARCH FOR PIVOT ELEMENT                                  CDMT 630
C      AMAX = (0DO,0DO)                                          CDMT 640
C                                                                CDMT 650
C      DO 7 J=1,N                                               CDMT 660
C      IF ( IPIVOT(J)-1) 3,7,3                                  CDMT 670
C                                                                CDMT 680
C      3 DO 6 K=1,N                                              CDMT 690
C      IF ( IPIVOT(K)-1) 4,6,21                                  CDMT 700
C      4 TEMP = AMAX*DCONJG(AMAX)-A(J,K)*DCONJG(A(J,K))          CDMT 710
C      IF (TEMP) 5,5,6                                           CDMT 720
C      5 IROW = J                                                 CDMT 730
C                                                                CDMT 740
C                                                                CDMT 750
C                                                                CDMT 760

```



```

ICOLU = K
AMAX = A(J,K)
6 CONTINUE
7 CCNTINUE
  IPIVOT(ICOLU) = IPIVOT(ICOLU)+1
  INTERCHANGE ROWS TO PUT PIVOT ELEMENT ON DIAGONAL
  IF (IROW-ICCLU) 8,10,8
8 CONTINUE
  DC 9 L=1,N
  SWAP = A(IROW,L)
  A(IROW,L) = A(ICOLU,L)
  A(ICOLU,L) = SWAP
  SWAP = ALPHA(IROW)
  ALPHA(IROW) = ALPHA(ICOLU)
  ALPHA(ICOLU) = SWAP
10 INDEX(I,1) = IROW
  INDEX(I,2) = ICOLU
  PIVOT(I) = A(ICOLU, ICOLU)
  U = PIVOT(I)
  TEMP = PIVOT(I)*DCONJG(PIVOT(I))
  IF (TEMP) 11,20,11
    DIVIDE PIVOT ROW BY PIVOT ELEMENT
11 A(ICOLU,ICOLU) = (1CO,ODO)
  DC 12 L=1,N
  U = PIVOT(I)
12 A(ICOLU,L) = A(ICOLU,L)/U
  REDUCE NON-PIVOT ROWS
  CO 15 L=1,N
  IF (L1-ICOLU) 13,15,13
  T = A(L1,ICOLU)
13 A(L1,ICOLU) = (OCO,ODO)
  CO 14 L=1,N
  U = A(ICOLU,L)
14 A(L1,L) = A(L1,L)-U*T

```


C	15	CONTINUE	CDMT1250
C			CDMT1260
C	16	CONTINUE	CDMT1270
C			CDMT1280
C		INTERCHANGE COLUMNS	CDMT1290
C			CDMT1300
C			CDMT1310
C			CDMT1320
C			CDMT1330
	19	I=1,N	CDMT1340
		L = N+1-1	CDMT1350
		IF (INDEX(L,1)-INDEX(L,2))	CDMT1360
	17	JROW = INDEX(L,1)	CDMT1370
		JCOLUMN = INDEX(L,2)	CDMT1380
C			CDMT1390
	18	DO 18 K=1,N	CDMT1400
		SWAP = A(K,JROW)	CDMT1410
		A(K,JROW) = A(K,JCOLUMN)	CDMT1420
		A(K,JCOLUMN) = SWAP	CDMT1430
	18	CONTINUE	CDMT1440
C			CDMT1450
C	19	CONTINUE	CDMT1460
			CDMT1470
		RETURN	CDMT1480
	20	WRITE (6,22)	CDMT1490
		IERR = 9999	CDMT1500
	21	RETURN	CDMT1510
C	22	FORMAT (20H MATRIX IS SINGULAR)	CDMT1520
		END	CDMT1530
C			CDMT1540
C	 SUBROUTINE MULM(X1,X2,N,MDIM,TEMPV).....	MULM 10
C		PURPOSE	MULM 20
C		PERFORMS THE MATRIX MULTIPLICATION OF A SQUARE MATRIX BY A	MULM 30
C		SQUARE MATRIX. THE RESULT IS RETURNED IN MATRIX X1.	MULM 40
C		USAGE	MULM 50
C		CALL MULM(X1,X2,N,MDIM,TEMPV)	MULM 60
C		DESCRIPTION OF PARAMETERS	MULM 70
C		X1 - THE MULTIPLYING MATRIX ON INPUT AND THE RESULTANT PRODUCT	MULM 80
C		ON OUTPUT.	MULM 90
C			MULM 100
C			MULM 110
C			MULM 120
C			MULM 130
C			MULM 140
C			MULM 150
C			MULM 160

[illegible]

.....SUBROUTINE DSPLIT(N,MDIM,A,AR,AI).....	DSPL	10
	DSPL	20
	DSPL	30
	DSPL	40
	DSPL	50
DSPLIT TAKES A MATRIX OF COMPLEX*16 NUMBERS AND	DSPL	60
SPLITS IT INTO TWO MATRICES, ONE CONTAINING THE REAL	DSPL	70
PART OF THE ORIGINAL MATRIX, AND ONE CONTAINING THE	DSPL	80
IMAGINARY PART.	DSPL	90
	DSPL	100
USAGE	DSPL	110
CALL DSPLIT(N,MDIM,A,AREAL,AIMAG)	DSPL	120
DESCRIPTION OF PARAMETERS	DSPL	130
	DSPL	140
	DSPL	150
N - THE SIZE OF THE MATRIX A, AN N BY N SQUARE	DSPL	160
MATRIX.	DSPL	170
MDIM - THE COLUMN DIMENSION OF MATRIX A	DSPL	180
	DSPL	190
A - THE INPUT MATRIX. MUST BE DIMENSIONED MDIM BY	DSPL	200
AT LEAST N IN THE CALLING PROGRAM (COMPLEX*16)	DSPL	210
	DSPL	220
AREAL,AIMAG - THE OUTPUT MATRICES CONTAINING THE	DSPL	230
REAL AND IMAGINARY PARTS, RESPECTIVELY, OF	DSPL	240
MATRIX A. MUST BE DIMENSIONED (MDIM,MDIM) IN THE	DSPL	250
CALLING PROGRAM.	DSPL	260
	DSPL	270
	DSPL	280
	DSPL	290
NOTES....	DSPL	300
	DSPL	310
MATRIX A AND MATRIX AREAL MAY OVERLAP IF THEY ARE	DSPL	320
DIMENSIONED IN THE CALLING PROGRAM AS FOLLOWS...	DSPL	330
	DSPL	340
COMPLEX*16 A(MDIM,MDIM)	DSPL	350
REAL*8 AREAL(MDIM,MDIM),AIMAG(MDIM,MDIM)	DSPL	360
EQUIVALENCE(A(1,1),AREAL(1,1))	DSPL	370
	DSPL	380
OTHER ROUTINES NEEDED	DSPL	390
	DSPL	400
NONE	DSPL	410
	DSPL	420
	DSPL	430
	DSPL	440
	DSPL	450
SUBROUTINE DSPLIT (N,MDIM,A,AR,AI)	DSPL	460
REAL *8A(2,MDIM,MDIM),AR(MDIM,MDIM),AI(MDIM,MDIM)	DSPL	470
	DSPL	480

DSPL 490
DSPL 500
DSPL 510
DSPL 520
DSPL 530
DSPL 540
DSPL 550
DSPL 560
DSPL 570
DSPL 580

DO 1 J=1,N
DO 1 I=1,N
AR(I,J) = A(1,I,J)
1 AI(I,J) = A(2,I,J)

RETURN
END

SUBROUTINE EBALAC (AR,AI,N,IA,K,L,D)

-----D-----LIBRARY 1-----

FUNCTION

USAGE
PARAMETERS
AR
AI

N

IA

K

L

D

PRECISION
LANGUAGE

-----LATEST REVISION

MARCH 9, 1977

SUBROUTINE EBALAC (AR,AI,N,IA,K,L,D)

DIMENSION

AR(IA,1),AI(IA,1),D(N)

EBAC0010
EBAC0020
EBAC0030
EBAC0040
EBAC0050
EBAC0060
EBAC0070
EBAC0080
EBAC0090
EBAC0100
EBAC0110
EBAC0120
EBAC0130
EBAC0140
EBAC0150
EBAC0160
EBAC0170
EBAC0180
EBAC0190
EBAC0200
EBAC0210
EBAC0220
EBAC0230
EBAC0240
EBAC0250
EBAC0260
EBAC0270
EBAC0280
EBAC0290
EBAC0300
EBAC0310
EBAC0320
EBAC0330
EBAC0340
EBAC0350
EBAC0360

- BALANCES A COMPLEX GENERAL MATRIX AND ISOLATES
EIGENVALUES WHENEVER POSSIBLE.
- CALL EBALAC (AR,AI,N,IA,K,L,D)
- INPUT/OUTPUT MATRICES OF DIMENSION N BY N.
ON INPUT, AR AND AI CONTAIN THE REAL
AND IMAGINARY PARTS, RESPECTIVELY, OF
THE COMPLEX MATRIX OF ORDER N TO BE
BALANCED. ON OUTPUT, AR AND AI CONTAIN THE
REAL AND IMAGINARY PARTS OF THE
TRANSFORMED MATRIX.
- INPUT VARIABLE CONTAINING THE ORDER
OF THE MATRIX A = (AR,AI) TO BE BALANCED.
- INPUT VARIABLE CONTAINING THE ROW DIMENSION OF
AR AND AI IN THE CALLING PROGRAM.
- OUTPUT INTEGERS CONTAINING THE BOUNDARY
INDICES FOR THE BALANCED MATRIX A = (AR,AI)
SUCH THAT
AR(I,J) = 0. AND AI(I,J) = 0. IF
(1) I IS GREATER THAN J AND
(2) J = 1,...,K-1 OR
I = L+1,...,N
- OUTPUT VECTOR OF LENGTH N CONTAINING
INFORMATION DETERMINING THE PERMUTATIONS
USED AND THE SCALING FACTORS.
- SINGLE/DOUBLE
- FORTRAN


```

C
C
      M = L
      IEXC = 1
      GO TO 5
40 CONTINUE
   GO TO 50

45 K = K+1
50 DO 60 J = K,L
   DO 55 I = K,L
     IF (I.EQ.J) GC TO 55
     IF (AR(I,J) .NE. ZERO .OR. AI(I,J) .NE. ZERO) GO TO 60
55 CONTINUE
   M = K
   IEXC = 2
   GO TO 5
60 CONTINUE

C
C
      DO 65 I = K,L
      D(I) = ONE
65 CONTINUE

70 NOCONV = .FALSE.
   DO 110 I = K,L
     C = ZERO
     R = ZERO
     DO 75 J = K,L
       IF (J.EQ.I) GO TO 75
       C = C+DABS(AR(J,I))+DABS(AI(J,I))
       R = R+DABS(AR(I,J))+DABS(AI(I,J))
75 CONTINUE
     G = R*RRADIX
     F = ONE
     S = C+R
     IF (C .GE. G) GO TO 85
     F = F*RADIX
     C = C*B2
     GO TO 80
85 G = R*RACIX
   IF (C .LT. G) GO TO 95
   F = F*RRADIX
   C = C*RB2
   GO TO 90
95 IF (C+R)/F .GE. PT95*S) GO TO 110
   G = ONE/F
   D(I) = D(I)*F
      BALANCE
      GO TO 110

```

EBAC 0870
 EBAC 0880
 EBAC 0890
 EBAC 0900
 EBAC 0910
 EBAC 0920
 EBAC 0930
 EBAC 0940
 EBAC 0950
 EBAC 0960
 EBAC 0970
 EBAC 0980
 EBAC 0990
 EBAC 1000
 EBAC 1010
 EBAC 1020
 EBAC 1030
 EBAC 1040
 EBAC 1050
 EBAC 1060
 EBAC 1070
 EBAC 1080
 EBAC 1090
 EBAC 1100
 EBAC 1110
 EBAC 1120
 EBAC 1130
 EBAC 1140
 EBAC 1150
 EBAC 1160
 EBAC 1180
 EBAC 1200
 EBAC 1210
 EBAC 1220
 EBAC 1230
 EBAC 1240
 EBAC 1250
 EBAC 1260
 EBAC 1270
 EBAC 1280
 EBAC 1290
 EBAC 1300
 EBAC 1310
 EBAC 1320
 EBAC 1330
 EBAC 1340
 EBAC 1350
 EBAC 1360


```

NOCONV = .TRUE.
DO 100 J = K, N
  AR(I, J) = AR(I, J)*G
  AI(I, J) = AI(I, J)*G
100 CONTINUE
DO 105 J = 1, L
  AR(J, I) = AR(J, I)*F
  AI(J, I) = AI(J, I)*F
105 CONTINUE
110 CONTINUE
115 IF (NOCONV) GO TO 70
  RETURN
END

```

```

SUBROUTINE EHESCC (AR, AI, K, L, N, IA, ID)

```

```

-----D-----LIBRARY 1-----

```

```

FUNCTION

```

```

USAGE
PARAMETERS AR

```

```

-- REDUCTION OF A COMPLEX MATRIX TO COMPLEX
  UPPER HESSENBERG FORM.
-- CALL EHESCC(AR, AI, K, L, N, IA, ID)
-- INPUT/OUTPUT MATRIX OF DIMENSION N BY N. OF
  ON INPUT CONTAINS THE REAL COMPONENTS OF
  THE MATRIX TO BE REDUCED.
  ON OUTPUT CCNTAINS THE REAL COMPONENTS
  OF THE REDUCED HESSENBERG FORM IN THE
  UPPER TRIANGULAR PORTION (INCLUDING MAIN
  AND SUB-DIAGONAL) AND THE DETAILS OF
  THE REDUCTION IN THE LOWER TRIANGULAR
  PORTION.

```

```

AI -- INPUT/OUTPUT MATRIX OF DIMENSION N BY N
  CONTAINING THE IMAGINARY COUNTERPARTS
  TO AR, ABOVE.
K -- INPUT SCALAR CONTAINING THE ROW AND COLUMN
  INDEX OF THE STARTING ELEMENT TO BE
  REDUCED BY ROW SCALING. FOR UNBALANCED
  MATRICES SET K = 1.
L -- INPUT SCALAR CONTAINING THE ROW AND
  COLUMN INDEX OF THE LAST ELEMENT TO BE
  REDUCED BY ROW SCALING. FOR UNBALANCED
  MATRICES SET L = N.
N -- INPUT SCALAR CONTAINING THE ORDER OF
  THE MATRIX TO BE REDUCED.
IA -- INPUT SCALAR CONTAINING ROW DIMENSION
  OF AR AND AI IN THE CALLING PROGRAM.
ID -- OUTPUT VECTOR OF LENGTH L CONTAINING
  DETAILS OF THE TRANSFORMATIONS.
-- SINGLE/DOUBLE

```

```

PRECISION

```

```

EBAC1370
EBAC1380
EBAC1390
EBAC1400
EBAC1410
EBAC1420
EBAC1430
EBAC1440
EBAC1450
EBAC1460
EBAC1470
EBAC1480
EBAC1490

```

```

EHEC0010
EHEC0020
EHEC0030
EHEC0040
EHEC0050
EHEC0060
EHEC0070
EHEC0080
EHEC0090
EHEC0100
EHEC0110
EHEC0120
EHEC0130
EHEC0140
EHEC0150
EHEC0160
EHEC0170
EHEC0180
EHEC0190
EHEC0200
EHEC0210
EHEC0220
EHEC0230
EHEC0240
EHEC0250
EHEC0260
EHEC0270
EHEC0280
EHEC0290
EHEC0300
EHEC0310
EHEC0320
EHEC0330
EHEC0340

```



```

C      LANGUAGE      - FORTRAN
C-----
C      LATEST REVISION - FEBRUARY 7, 1973
C
C      SUBROUTINE EHESSC (AR, AI, K, L, N, IA, ID)
C
C      DIMENSION
C      DOUBLE PRECISION
C      COMPLEX*16
C      EQUIVALENCE
C
C      DATA
C      LA=L-1
C      KPI=K+1
C      IF (LA .LT. KPI) GO TO 45
C      DC 40 M=KPI, LA
C      I=M
C      XR=ZERO
C      XI=ZERO
C      DO 5 J=M, L
C      IF (DABS(AR(J, M-1))+DABS(AI(J, M-1)) .LE. DABS(XR)+DABS(XI))
C      GO TO 5
C      XR=AR(J, M-1)
C      XI=AI(J, M-1)
C      I=J
C      CONTINUE
C      ID(M)=I
C      IF (I .EQ. M) GO TO 20
C
C      MM1=M-1
C      DO 10 J=MM1, N
C      YR=AR(I, J)
C      AR(I, J)=AR(M, J)
C      AR(M, J)=YR
C      YI=AI(I, J)
C      AI(I, J)=AI(M, J)
C      AI(M, J)=YI
C      CONTINUE
C      DO 15 J=1, L
C      YR=AR(J, I)
C      AR(J, I)=AR(J, M)
C      AR(J, M)=YR
C      YI=AI(J, I)
C      AI(J, I)=AI(J, M)
C      AI(J, M)=YI
C      CONTINUE
C
C      END INTERCHANGE
C
EHEC0350
EHEC0360
EHEC0370
EHEC0380
EHEC0390
EHEC0400
EHEC0410
EHEC0420
EHEC0430
EHEC0440
EHEC0450
EHEC0460
EHEC0470
EHEC0490
EHEC0500
EHEC0510
EHEC0520
EHEC0530
EHEC0540
EHEC0550
EHEC0560
EHEC0570
EHEC0580
EHEC0610
EHEC0620
EHEC0630
EHEC0640
EHEC0650
EHEC0660
EHEC0670
EHEC0680
EHEC0690
EHEC0700
EHEC0710
EHEC0720
EHEC0730
EHEC0740
EHEC0750
EHEC0760
EHEC0770
EHEC0780
EHEC0790
EHEC0800
EHEC0810
EHEC0820
EHEC0830
EHEC0840
EHEC0850
EHEC0860

```



```

20 IF (XR .EQ. ZERO .AND. XI .EQ. ZERO) GO TO 40
   MP1=M+1
   DO 35 I=MP1,L
     YR=AR(I,M-1)
     YI=AI(I,M-1)
     IF (YR .EQ. ZERO .AND. YI .EQ. ZERO) GO TO 35
     Y=Y/X
     AR(I,M-1)=YR
     AI(I,M-1)=YI
     DO 25 J=M,N
       CONTINUE
       DO 30 J=1,L
         AR(J,M)+YR*AR(J,I)-YI*AI(J,I)
         AI(J,M)+YI*AR(J,I)+YI*AI(J,I)
       CONTINUE
     CONTINUE
   CONTINUE
30 RETURN
35 END
40

```

EHEC0870
 EHEC0880
 EHEC0890
 EHEC0900
 EHEC0910
 EHEC0920
 EHEC0930
 EHEC0940
 EHEC0970
 EHEC0950
 EHEC0980
 EHEC0960
 EHEC0990
 EHEC1000
 EHEC1010
 EHEC1020
 EHEC1030
 EHEC1040
 EHEC1050
 EHEC1060
 EHEC1070

```

C-----D-----LIBRARY 1-----
SUBROUTINE ELRH2C (HR,HI,K,L,N,IH,WR,WI,ZR,ZI,ID,INFER,IER)

FUNCTION
  - COMPUTE THE EIGENVALUES AND EIGENVECTORS OF
  - A COMPLEX UPPER HESSENBERG MATRIX AND
  - BACK TRANSFORM THE EIGENVECTORS.
  - CALL ELRH2C (FR,HI,K,L,N,IH,WR,WI,ZR,ZI,ID,
  - INFER,IER)
  - INPUT MATRIX OF DIMENSION N BY N CONTAINING
  - THE REAL COMPONENTS OF THE COMPLEX
  - HESSENBERG MATRIX. HR IS DESTROYED ON
  - OUTPUT.
  - INPUT MATRIX OF DIMENSION N BY N CONTAINING
  - THE IMAGINARY COUNTERPARTS TO HR, ABOVE.
  - HI IS DESTROYED ON OUTPUT.
  - INPUT SCALAR CONTAINING THE LOWER BOUNDARY
  - INDEX FOR THE INPUT MATRIX.
  - FOR UNBALANCED MATRICES SET K = 1.
  - INPUT SCALAR CONTAINING THE UPPER BOUNDARY
  - INDEX FOR THE INPUT MATRIX.
  - FOR UNBALANCED MATRICES SET L = N.
  - INPUT SCALAR CONTAINING THE ORDER OF THE
  - HESSENBERG MATRIX AND THE EIGENVECTOR
  - MATRIX.

PARAMETERS FR HI K L N

C-----D-----LIBRARY 1-----
ELRH2C-----D-----LIBRARY 1-----

```

ELR20010
 ELR20020
 ELR20030
 ELR20040
 ELR20050
 ELR20060
 ELR20070
 ELR20080
 ELR20090
 ELR20100
 ELR20110
 ELR20120
 ELR20130
 ELR20140
 ELR20150
 ELR20160
 ELR20170
 ELR20180
 ELR20190
 ELR20200
 ELR20210
 ELR20220
 ELR20230
 ELR20240
 ELR20250

IH - INPUT SCALAR CONTAINING THE ROW DIMENSION
 OF MATRICES HR, HI, ZR AND ZI IN THE
 CALLING PROGRAM.
 WR - OUTPUT VECTOR OF LENGTH N CONTAINING THE REAL
 COMPONENTS OF THE EIGENVALUES.
 WI - OUTPUT VECTOR OF LENGTH N CONTAINING THE
 IMAGINARY COMPONENTS OF THE EIGENVALUES.
 ZR - OUTPUT MATRIX OF DIMENSION N BY N CONTAINING
 THE REAL COMPONENTS OF THE EIGENVECTORS.
 ZI - OUTPUT MATRIX OF DIMENSION N BY N CONTAINING
 THE EIGENVECTORS ARE NOT NORMALIZED.
 ID - INPUT VECTOR OF COUNTERPARTS TO ZR, ABOVE.
 INFER - OUTPUT SCALAR CONTAINING THE INDEX OF THE
 EIGENVALUE WHICH GENERATED THE TERMINAL
 ERROR (SEE DESCRIPTION OF IER, BELOW).
 IER - ERROR PARAMETER

N = 1 INDICATES THE EIGENVALUE RECORDED
 IN THE OUTPUT PARAMETER, INFER,
 COULD NOT BE DETERMINED AFTER 30
 ITERATIONS. IF THE J-TH EIGENVALUE
 COULD NOT BE SO DETERMINED,
 THEN THE EIGENVALUES J+1, J+2, ..., N
 SHOULD BE CORRECT.

PRECISION - SINGLE/DOUBLE
 REQD. IMSL ROUTINES - UERTST
 LANGUAGE - FORTRAN

LATEST REVISION - APRIL 5, 1977

SUBROUTINE ELRH2C (HR, HI, K, L, N, IH, WR, WI, ZR, ZI, ID, INFER, IER)

DIMENSION
 DIMENSION
 COMPLEX*16
 DCUBLE PRECISION
 DCUBLE PRECISION
 DCUBLE PRECE
 EQUIVALENCE
 (X, Y, Z)
 (Y, T2(1), XR), (T1(2), XI),
 (Z, T3(1), ZZR), (T3(2), ZZI)
 ZERO, ONE, TWO/0.000, 1.000, 2.000/

1
 2 DATA

ELR20260
 ELR20270
 ELR20280
 ELR20290
 ELR20300
 ELR20310
 ELR20320
 ELR20330
 ELR20340
 ELR20350
 ELR20360
 ELR20370
 ELR20380
 ELR20390
 ELR20400
 ELR20410
 ELR20420
 ELR20430
 ELR20440
 ELR20450
 ELR20460
 ELR20470
 ELR20480
 ELR20490
 ELR20500
 ELR20510
 ELR20520
 ELR20530
 ELR20540
 ELR20550
 ELR20560
 ELR20570
 ELR20580
 ELR20590
 ELR20600
 ELR20610
 ELR20620
 ELR20630
 ELR20640
 ELR20650
 ELR20660
 ELR20680
 ELR20690
 ELR20700
 ELR20710
 ELR20720
 ELR20730
 ELR20740


```

C          DATA
C          IER=0
C          INFER=0
C          TR=ZERO
C          TI=ZERO
C          DC 5 I=1,N
C          DO 3 J=1,N
C             ZR(I,J)=ZERO
C             ZI(I,J)=ZERO
C          CONTINUE
C          ZR(I,I) = ONE
C          CONTINUE
C
C          IEND=L-K-1
C          IF (IEND .LE. 0) GO TO 25
C
C          DO 20 II=1,IEND
C             I=L-II
C             IP1=I+1
C             IM1=I-1
C             DO 10 M=IP1,L
C                ZR(M,I)=HR(M,IM1)
C                ZI(M,I)=HI(M,IM1)
C            CONTINUE
C            J=ID(I)
C            IF (I .EQ. J) GO TO 20
C            DO 15 M=I,L
C                ZR(I,M)=ZR(J,M)
C                ZI(I,M)=ZI(J,M)
C                ZR(J,M)=ZERO
C                ZI(J,M)=ZEROC
C            CONTINUE
C            ZR(J,I)=ONE
C          CONTINUE
C          DO 30 I=1,N
C             IF (I .GE. K .AND. I .LE. L) GO TO 30
C             WR(I)=HR(I,I)
C             WI(I)=HI(I,I)
C          CCNTINUE
C          NN=L
C
C          IF (NN .LT. K) GO TO 150
C          ITS=0
C          NNM1=NN-1
C          NNM2=NN-2
C
C          FORM THE MATRIX OF ACCUMULATED
C          TRANSFORMATIONS FROM THE INFOR-
C          MATION LEFT BY ROUTINE 'EHESSC'
C
C          DO I=L-1,K+1,-1
C
C          SEARCH FOR NEXT EIGENVALUE

```

```

ELR20750
ELR20770
ELR20780
ELR20790
ELR20800
ELR20810
ELR20820
ELR20830
ELR20840
ELR20850
ELR20860
ELR20870
ELR20880
ELR20890
ELR20900
ELR20910
ELR20920
ELR20930
ELR20940
ELR20950
ELR20960
ELR20970
ELR20980
ELR20990
ELR21000
ELR21010
ELR21020
ELR21030
ELR21040
ELR21050
ELR21060
ELR21070
ELR21080
ELR21090
ELR21100
ELR21110
ELR21120
ELR21130
ELR21140
ELR21150
ELR21160
ELR21170
ELR21180
ELR21190
ELR21200
ELR21210
ELR21220
ELR21230

```



```

C      IF (NN .EQ. K) GO TO 50
C      LOOK FOR SINGLE SMALL SUB-DIAGONAL
C      ELEMENT
C      DO M=NN,K+1,-1
C      DO 45 KK=K,NNM1
C      M=NPL-KK
C      MM1=M-1
C      IF (DABS(HR(M,MM1))+DABS(HI(M,MM1)) .LE. EPS*(DABS(HR(MM1,MM1)) GO TO 55
C      +DABS(HI(MM1,MM1))+DABS(HR(M,M))+DABS(HI(M,M)))) GO TO 55
C      1 CONTINUE
C      45 M=K
C      IF (M .EQ. NN) GO TO 145
C      IF (ITS .EQ. 30) GO TO 205
C      IF (ITS .EQ. 10 .OR. ITS .EQ. 20) GO TO 60
C      SR=HR(NN,NN)
C      SI=HI(NN,NN)
C      XR=HR(NN,NN)*HR(NN,NNM1)-HI(NN,NN)*HI(NN,NNM1)
C      XI=HR(NN,NNM1)*HI(NN,NNM1)+HI(NN,NNM1)*HR(NN,NNM1)
C      IF (XR .EQ. ZERO .AND. XI .EQ. ZERO) GO TO 65
C      YR=(HR(NN,NNM1)-SR)/TWO
C      YI=(HI(NN,NNM1)-SI)/TWO
C      Z=CDSQRT(DCMPLX(YR**2-YI**2+XR,TWO*YR*YI+XI))
C      IF (YR*ZXR+YI*ZZI .LT. ZERO) Z=-Z
C      X=X/(Y+Z)
C      SR=SR-XR
C      SI=SI-XI
C      GO TO 65
C      60 SR=DABS(HR(NN,NNM1))+DABS(HR(NN,NNM1,NNM2))
C      SI=DABS(HI(NN,NNM1))+DABS(HI(NN,NNM1,NNM2))
C      65 DO 70 I=K,NN
C      HR(I,I)=HR(I,I)-SR
C      HI(I,I)=HI(I,I)-SI
C      70 CONTINUE
C      TR=TR+SR
C      TI=TI+SI
C      ITS=ITS+1
C      LOOK FOR TWO CONSECUTIVE SMALL
C      SUB-DIAGONAL ELEMENTS
C      XR=DABS(HR(NN,NNM1,NNM1))+DABS(HI(NN,NNM1,NNM1))
C      YR=DABS(HR(NN,NNM1))+DABS(HI(NN,NNM1))
C      ZZR=DABS(HR(NN,NN))+DABS(HI(NN,NN))
C      NNMJ=NNM1-M
C      IF (NNMJ .EQ. 0) GO TO 80
C      DO 75 NM=1,NNMJ
C      MM=NN-NM
C      DO MM=NN-1,M+1,-1

```

ELR21240
ELR21250
ELR21260
ELR21270
ELR21280
ELR21290
ELR21300
ELR21310
ELR21320
ELR21330
ELR21360
ELR21370
ELR21380
ELR21390
ELR21400
ELR21410
ELR21420
ELR21430
ELR21440
ELR21450
ELR21460
ELR21470
ELR21480
ELR21490
ELR21510
ELR21520
ELR21530
ELR21540
ELR21550
ELR21560
ELR21570
ELR21600
ELR21610
ELR21620
ELR21630
ELR21640
ELR21650
ELR21660
ELR21670
ELR21680
ELR21690
ELR21700
ELR21710
ELR21750
ELR21760
ELR21770
ELR21780
ELR21790


```

MMM1=MM-1
YI=YR
YR=DABS(HR(MM,MMM1))+DABS(HI(MM,MMM1))
XI=ZZR
ZZR=XR
XR=DABS(HR(MMM1,MMM1))+DABS(HI(MMM1,MMM1))
IF (YR .LE. EPS*ZZR/YI*(ZZR+XR+XI)) GO TO 85
75 CONTINUE
80 MM=M
C
85 MP1=MM+1
DO 110 I=MP1,NN
IM1=I-1
XR=HR(IM1,IM1)
XI=HI(IM1,IM1)
YR=HR(I,IM1)
YI=HI(I,IM1)
IF (DABS(XR)+DABS(XI) .GE. DABS(YR)+DABS(YI)) GO TO 95
INTERCHANGE ROWS OF HR AND HI
DO 90 J=IM1,N
ZZR=HR(IM1,J)
HR(IM1,J)=HR(I,J)
HR(I,J)=ZZR
ZZI=HI(IM1,J)
HI(IM1,J)=HI(I,J)
HI(I,J)=ZZI
CONTINUE
Z=X/Y
WR(I)=ONE
GO TO 100
95 Z=Y/X
WR(I)=-ONE
HR(I,IM1)=ZZR
HI(I,IM1)=ZZI
DO 105 J=I,N
HR(I,J)=HR(I,J)-ZZR*HR(IM1,J)+ZZI*HI(IM1,J)
HI(I,J)=HI(I,J)-ZZR*HI(IM1,J)+ZZI*HR(IM1,J)
CONTINUE
105 CONTINUE
110 CONTINUE
C
DO 140 J=MP1,NN
JM1=J-1
XR=HR(J,JM1)
XI=HI(J,JM1)
HR(J,JM1)=ZERO
HI(J,JM1)=ZERO
C
C

```

TRIANGULAR DECOMPOSITION H=L*R

COMPOSITION R*L=H

INTERCHANGE COLUMNS OF HR, HI,
ZR, AND ZI IF NECESSARY


```

IF (WR(J) .LE. ZERC) GO TO 125
DO 115 I=1,J
  ZZR=HR(I,JM1)
  HR(I,JM1)=HR(I,J)
  HR(I,J)=ZZR
  ZZI=HI(I,JM1)
  HI(I,JM1)=HI(I,J)
  HI(I,J)=ZZI
CONTINUE
115 DO 120 I=K,L
  ZZR=ZR(I,JM1)
  ZR(I,JM1)=ZR(I,J)
  ZR(I,J)=ZZR
  ZZI=ZI(I,JM1)
  ZI(I,JM1)=ZI(I,J)
  ZI(I,J)=ZZI
CONTINUE
120 CONTINUE
END INTERCHANGE COLUMNS
125 DO 130 I=1,J
  HR(I,JM1)=HR(I,JM1)+XR*HR(I,J)-XI*HI(I,J)
  HI(I,JM1)=HI(I,JM1)+XR*HI(I,J)+XI*HR(I,J)
CONTINUE
130 DO 135 I=K,L
  ZR(I,JM1)=ZR(I,JM1)+XR*ZR(I,J)-XI*ZI(I,J)
  ZI(I,JM1)=ZI(I,JM1)+XR*ZI(I,J)+XI*ZR(I,J)
CONTINUE
135 CONTINUE
END ACCUMULATE TRANSFORMATIONS
140 CONTINUE
GC TO 40
C
145 WR(NN)=HR(NN,NN)+TR
  WI(NN)=HI(NN,NN)+TI
  NN=NNM1
GO TO 35
C
150 IF (N.EQ. 1) GO TO 9005
  FNORM=ZERO
  DC 160 I=1,N
    FNORM=FNORM+DABS(WR(I))+DABS(WI(I))
    IF (I.EQ. N) GO TO 160
    IP1=I+1
    DO 155 J=IP1,N
      FNORM=FNORM+DABS(HR(I,J))+DABS(HI(I,J))
    CONTINUE
  155 CONTINUE
  160 IF (FNORM .EQ. ZERO) GO TO 9005

```

ALL ROOTS FOUND. BACKSUBSTITUTE TO
FIND VECTORS OF UPPER TRIANGULAR
FORM

ELR22310
ELR22320
ELR22330
ELR22340
ELR22350
ELR22360
ELR22370
ELR22380
ELR22390
ELR22400
ELR22410
ELR22420
ELR22430
ELR22440
ELR22450
ELR22460
ELR22470
ELR22480
ELR22490
ELR22500
ELR22510
ELR22520
ELR22530
ELR22540
ELR22550
ELR22560
ELR22570
ELR22580
ELR22590
ELR22600
ELR22610
ELR22620
ELR22630
ELR22640
ELR22650
ELR22660
ELR22670
ELR22680
ELR22690
ELR22700
ELR22710
ELR22720
ELR22730
ELR22740
ELR22750
ELR22760
ELR22780
ELR22790
ELR22800


```

C
NP2 = N+2
DO 180 NM=2,N
  NN=NP2-NM
  XR=WR(NN)
  XI=WI(NN)
  NNM1=NN-1
C
DO 175 II=1,NNM1
  I=NN-II
  ZZR=HR(I,NN)
  ZZI=HI(I,NN)
  IF (I.EQ. NNM1) GO TO 170
  IP1=I+1
  DO 165 J=IP1,NNM1
    ZZR=ZZR+HR(I,J)*HR(J,NN)-HI(I,J)*HI(J,NN)
    ZZI=ZZI+HR(I,J)*HI(J,NN)+HI(I,J)*HR(J,NN)
  C CONTINUE
  YR=XR-WR(I)
  YI=XI-WI(I)
  IF (YR.EQ. ZERO .AND. YI.EQ. ZERO) YR=EPS*FNORM
  Z=Z/Y
  HR(I,NN)=T3(1)
  HI(I,NN)=T3(2)
C CONTINUE
165
170
175 CONTINUE
180 CONTINUE
  NNM1=N-1
C
DO 190 I=1,NNM1
  IF (I.GE. K .AND. I.LE. L) GO TO 190
  IP1=I+1
  DO 185 J=IP1,N
    ZR(I,J)=HR(I,J)
    ZI(I,J)=HI(I,J)
  C CONTINUE
185 CONTINUE
190 IF (L.EQ. 0) GO TO 9005
C
  NPL=N+K
  DO 200 JJ=K,NNM1
    J=APL-JJ
    JM1=J-1
    DO 200 I=K,L
      ZZR=ZR(I,J)
C
C
C
C
DO NN=N,2,-1
ELR222810
ELR222820
ELR222830
ELR222840
ELR222850
ELR222860
ELR222870
ELR222880
ELR222890
ELR222900
ELR222910
ELR222920
ELR222930
ELR222940
ELR222950
ELR222960
ELR222970
ELR222980
ELR222990
ELR23000
ELR23010
ELR23020
ELR23030
ELR23040
ELR23050
ELR23060
ELR23070
ELR23080
ELR23090
ELR23100
ELR23110
ELR23120
ELR23130
ELR23140
ELR23150
ELR23160
ELR23170
ELR23180
ELR23190
ELR23200
ELR23210
ELR23220
ELR23230
ELR23240
ELR23250
ELR23260
ELR23270
ELR23280

```

MULTIPLY BY TRANSFORMATION MATRIX
TO GIVE VECTORS OF ORIGINAL FULL
MATRIX

DO J=N,K+1,-1

ELR233290
ELR233300
ELR233310
ELR233320
ELR233330
ELR233340
ELR233350
ELR233360
ELR233370
ELR233380
ELR233390
ELR233400
ELR233410
ELR233420
ELR233430
ELR233440
ELR233450
ELR233460
ELR233470

```

ZZI=ZI(I,J)
MM=JMI
IF (L.LT.J) MM=L
DO 195 M=K,MM
  ZZR=ZZR+ZR(I,M)*HR(M,J)-ZI(I,M)*HI(M,J)
  ZZI=ZZI+ZR(I,M)*HI(M,J)+ZI(I,M)*HR(M,J)
195 CONTINUE
  ZR(I,J)=ZZR
  ZI(I,J)=ZZI
200 CONTINUE
  GO TO 9005
C
205 IER=129
  INFER=NN
9000 CONTINUE
  CALL UERTST (IER,6ELRH2C)
9005 RETURN
      END

```

SET ERROR - NO CONVERGENCE TO AN
EIGENVALUE AFTER 30 ITERATIONS

EBBC0010
EBBC0020
EBBC0030
EBBC0040
EBBC0050
EBBC0060
EBBC0070
EBBC0080
EBBC0090
EBBC0100
EBBC0110
EBBC0120
EBBC0130
EBBC0140
EBBC0150
EBBC0160
EBBC0170
EBBC0180
EBBC0190
EBBC0200
EBBC0210
EBBC0220
EBBC0230
EBBC0240
EBBC0250
EBBC0260
EBBC0270

```

SUBROUTINE EBBCKC (ZR,ZI,N,IZ,K,L,M,D)
C-----LIBRARY 1-----
C
C FUNCTION
C
C USAGE
C
C PARAMETERS
C
C ZR
C
C ZI
C
C N
C
C IZ
C
C K
C
C L
C
C M
C
C D
C-----
      - BACKTRANSFORM THE EIGENVECTORS OF A BALANCED
      - COMPLEX GENERAL MATRIX.
      - CALL EBBCKC (ZR,ZI,N,IZ,K,L,M,D)
      - INPUT/OUTPUT MATRICES OF DIMENSION N BY M.
      - ON INPUT, THE FIRST M COLUMNS OF ZR AND
      - ZI CONTAIN THE REAL AND IMAGINARY PARTS,
      - RESPECTIVELY, OF THE EIGENVECTORS TO BE
      - BACK TRANSFORMED. ON OUTPUT, THESE M
      - COLUMNS CONTAIN THE REAL AND IMAGINARY
      - PARTS OF THE TRANSFORMED EIGENVECTORS.
      - INPUT SCALAR CONTAINING THE NUMBER OF
      - ROWS IN THE MATRIX Z = (ZR,ZI). N MUST
      - NOT BE GREATER THAN IZ.
      - INPUT SCALAR CONTAINING THE ROW DIMENSION
      - OF MATRICES ZR AND ZI IN THE CALLING
      - PROGRAM.
      - INPUT SCALARS CONTAINING THE BOUNDARY
      - INDICES FOR THE BALANCED MATRIX. K AND L
      - ARE TWO OUTPUT PARAMETERS FROM IMSL ROUTINE
      - EBBALC.
      - INPUT SCALAR CONTAINING THE NUMBER OF COLUMNS
      - OF Z = (ZR,ZI) TO BE BACK TRANSFORMED.
      - INPUT VECTOR OF LENGTH N CONTAINING THE

```



```

10 EIGFCN JOB (1719,0947,AX74), 'SMC 1882', TIME=2
20 // EXEC FORTCLGW
30 // FORT.SYSIN DD *
40
50
60
70
80
90
100
110
120
130
140
150
160
170
180
190
200
210
220
230
240
250
260
270
280
290
300
310
320
330
340
350
360
370
380
390
400
410
420
430
440
450
460
470
480
490
500
510
520
530
540
550
560
570
580
590
600
610
620
630
640
650
660
670
680
690
700
710
720
730
740
750
760
770
780
790
800
810
820
830
840
850
860
870
880
890
900
910
920
930
940
950
960
970
980
990
1000
1010
1020
1030
1040
1050
1060
1070
1080
1090
1100
1110
1120
1130
1140
1150
1160
1170
1180
1190
1200
1210
1220
1230
1240
1250
1260
1270
1280
1290
1300
1310
1320
1330
1340
1350
1360
1370
1380
1390
1400
1410
1420
1430
1440
1450
1460
1470
1480
1490
1500
1510
1520
1530
1540
1550
1560
1570
1580
1590
1600
1610
1620
1630
1640
1650
1660
1670
1680
1690
1700
1710
1720
1730
1740
1750
1760
1770
1780
1790
1800
1810
1820
1830
1840
1850
1860
1870
1880
1890
1900
1910
1920
1930
1940
1950
1960
1970
1980
1990
2000
2010
2020
2030
2040
2050
2060
2070
2080
2090
2100
2110
2120
2130
2140
2150
2160
2170
2180
2190
2200
2210
2220
2230
2240
2250
2260
2270
2280
2290
2300
2310
2320
2330
2340
2350
2360
2370
2380
2390
2400
2410
2420
2430
2440
2450
2460
2470
2480
2490
2500
2510
2520
2530
2540
2550
2560
2570
2580
2590
2600
2610
2620
2630
2640
2650
2660
2670
2680
2690
2700
2710
2720
2730
2740
2750
2760
2770
2780
2790
2800
2810
2820
2830
2840
2850
2860
2870
2880
2890
2900
2910
2920
2930
2940
2950
2960
2970
2980
2990
3000
3010
3020
3030
3040
3050
3060
3070
3080
3090
3100
3110
3120
3130
3140
3150
3160
3170
3180
3190
3200
3210
3220
3230
3240
3250
3260
3270
3280
3290
3300
3310
3320
3330
3340
3350
3360
3370
3380
3390
3400
3410
3420
3430
3440
3450
3460
3470
3480
3490
3500
3510
3520
3530
3540
3550
3560
3570
3580
3590
3600
3610
3620
3630
3640
3650
3660
3670
3680
3690
3700
3710
3720
3730
3740
3750
3760
3770
3780
3790
3800
3810
3820
3830
3840
3850
3860
3870
3880
3890
3900
3910
3920
3930
3940
3950
3960
3970
3980
3990
4000
4010
4020
4030
4040
4050
4060
4070
4080
4090
4100
4110
4120
4130
4140
4150
4160
4170
4180
4190
4200
4210
4220
4230
4240
4250
4260
4270
4280
4290
4300
4310
4320
4330
4340
4350
4360
4370
4380
4390
4400
4410
4420
4430
4440
4450
4460
4470
4480
4490
4500
4510
4520
4530
4540
4550
4560
4570
4580
4590
4600
4610
4620
4630
4640
4650
4660
4670
4680
4690
4700
4710
4720
4730
4740
4750
4760
4770
4780
4790
4800
4810
4820
4830
4840
4850
4860
4870
4880
4890
4900
4910
4920
4930
4940
4950
4960
4970
4980
4990
5000
5010
5020
5030
5040
5050
5060
5070
5080
5090
5100
5110
5120
5130
5140
5150
5160
5170
5180
5190
5200
5210
5220
5230
5240
5250
5260
5270
5280
5290
5300
5310
5320
5330
5340
5350
5360
5370
5380
5390
5400
5410
5420
5430
5440
5450
5460
5470
5480
5490
5500
5510
5520
5530
5540
5550
5560
5570
5580
5590
5600
5610
5620
5630
5640
5650
5660
5670
5680
5690
5700
5710
5720
5730
5740
5750
5760
5770
5780
5790
5800
5810
5820
5830
5840
5850
5860
5870
5880
5890
5900
5910
5920
5930
5940
5950
5960
5970
5980
5990
6000
6010
6020
6030
6040
6050
6060
6070
6080
6090
6100
6110
6120
6130
6140
6150
6160
6170
6180
6190
6200
6210
6220
6230
6240
6250
6260
6270
6280
6290
6300
6310
6320
6330
6340
6350
6360
6370
6380
6390
6400
6410
6420
6430
6440
6450
6460
6470
6480
6490
6500
6510
6520
6530
6540
6550
6560
6570
6580
6590
6600
6610
6620
6630
6640
6650
6660
6670
6680
6690
6700
6710
6720
6730
6740
6750
6760
6770
6780
6790
6800
6810
6820
6830
6840
6850
6860
6870
6880
6890
6900
6910
6920
6930
6940
6950
6960
6970
6980
6990
7000
7010
7020
7030
7040
7050
7060
7070
7080
7090
7100
7110
7120
7130
7140
7150
7160
7170
7180
7190
7200
7210
7220
7230
7240
7250
7260
7270
7280
7290
7300
7310
7320
7330
7340
7350
7360
7370
7380
7390
7400
7410
7420
7430
7440
7450
7460
7470
7480
7490
7500
7510
7520
7530
7540
7550
7560
7570
7580
7590
7600
7610
7620
7630
7640
7650
7660
7670
7680
7690
7700
7710
7720
7730
7740
7750
7760
7770
7780
7790
7800
7810
7820
7830
7840
7850
7860
7870
7880
7890
7900
7910
7920
7930
7940
7950
7960
7970
7980
7990
8000
8010
8020
8030
8040
8050
8060
8070
8080
8090
8100
8110
8120
8130
8140
8150
8160
8170
8180
8190
8200
8210
8220
8230
8240
8250
8260
8270
8280
8290
8300
8310

```



```

C      COMPUTE UPPRIME'S
C      DEL = 1D0/DFLOAT(N+1)
C      ETA(1) = 0.0D0
C      QPRIM(1) = 1.795918367D0*QPRIM(2)-1.24781341D0*QPRIM(3)+0.60641399
14D0*QPRIM(4)-0.17784256D0*QPRIM(5)+0.023323615D0*QPRIM(6)
C      UPPRIM(1) = 2D0*QPRIM(1)
C      CALL COEFNT (ETA(2),AMDA,COEF,KSET)
C      DQPRIM(2) = 2D0*(-QPRIM(2)+QPRIM(3))/(3D0*DEL)
C      DQPRIM(2) = COEF*DQPRIM(2)
C      UPPRIM(2) = 2D0*QPRIM(2)+ETA(2)*DQPRIM(2)
C      CALL COEFNT (ETA(3),AMDA,COEF,KSET)
C      DQPRIM(3) = 4D0*(-QPRIM(2)+QPRIM(3))/(3D0*DEL)
C      DQPRIM(3) = COEF*DQPRIM(3)
C      UPPRIM(3) = 2D0*QPRIM(3)+ETA(3)*DQPRIM(3)
C      DO 2 I=4,N
C      CALL COEFNT (ETA(I),AMDA,COEF,KSET)
C      DQPRIM(I) = (QPRIM(I+1)-QPRIM(I-1))/(2D0*DEL)
C      DQPRIM(I) = COEF*DQPRIM(I)
C      UPPRIM(I) = 2D0*QPRIM(I)+ETA(I)*DQPRIM(I)
2      CONTINUE
C      CALL COEFNT (ETA(N0),AMDA,COEF,KSET)
C      DQPRIM(N0) = -QPRIM(N)/(2D0*DEL)
C      DQPRIM(N0) = COEF*DQPRIM(N0)
C      UPPRIM(N0) = 2D0*QPRIM(N0)+ETA(N0)*DQPRIM(N0)
C      ETA(N1) = 1.0D0
C      UPPRIM(N1) = (0D0,0D0)
C      WRITE (6,10)
C      DETERMINE U VECTOR OF LARGEST MAGNITUDE
C      C = 0.0D0
C      DO 3 I=1,N1
C      IF (CDABS(UPPRIM(I)).GT.C) INDEX=I
C      IF (CDABS(UPPRIM(I)).GT.C) C=CDABS(UPPRIM(I))
3      CONTINUE
C      CONST = DCONJG(UPPRIM(INDEX))/C**2

```



```

C C C C C
NORMALIZE UPRIMES'S AND SPLIT INTO REAL & IMAGINARY VECTORS
      DO 4 I=1,N1
        UP(I) = CONST*UPRIM(I)
        UR(I) = UP(I)
        UI(I) = (OD0,-1D0)*UP(I)
      4 CONTINUE
C C C C C
      CONVERT U'S AND ETA'S TO SINGLE PRECISION FCR PLOTG
      DO 5 I=1,N1
        RAD1(I) = ETA(I)
        UR1(I) = UR(I)
        UI1(I) = UI(I)
        WRITE(6,11) RAD1(I),UR1(I),UI1(I)
      5 CONTINUE
C C C C C
      PLOT RESULTS
      CALL PLOTG(RAD1,UR1,N1,1,1,1,'RADIUS',6,'PERTURBATION VELOCITY',
    $ 21,0,1,1,1,7,7.)
      CALL PLOTG(RAD1,UR1,N1,2,1,5,'RADIUS',6,'PERTURBATION VELOCITY',
    $ 21,0,1,1,1,7,7.)
      CALL CHART(N,SREY,AR,AI,SGAMMA,SLAMDA)
      CALL PLOT(0.0,0.0,999)
      STOP
C C C C C
      FORMAT (I2,3D20.10)
      6 FORMAT (F15.7,2(1PD20.10))
      7 FORMAT (I2)
      8 FORMAT (F15.7,2(1PD20.10))
      9 FORMAT (I1)
     10 FORMAT (' ',3F15.7)
     11 END
C C C C C
..... SUBROUTINE COEFNT(ETA,AMDA,COEF,KSET)..... COEF 10
C C C C C
PURPOSE--WHEN AN OFFSET MESH IS USED, THIS SUBROUTINE GENERATES
THE COEFFICIENT REQUIRED TO CONVERT DQ/DETA TO DQ/DR AND
CONVERTS THE UNIFORM ETA VALUE INTO THE NONUNIFORM R VALUE
C C C C C

```


[illegible]


```

3 COEF = 1D0
  RETURN
  END
COEF 560
COEF 570
COEF 580

C.....SUBROUTINE CHART(N,SREY,AR,AI,SGAMMA,SLAMDA).....
C
C.....PURPOSE
C      TO LABEL THE GRAPH WITH INFORMATION PERTAINING TO THE PLOT
C
C.....EXAMPLE OF THE CALLING ARGUMENT
C      CALL CHART(N,SREY,AR,AI,SGAMMA,SLAMDA)
C
C.....DESCRIPTION OF PARAMETERS
C      THE PARAMETERS ARE SELF-EXPLANATORY AND MUST BE IN SINGLE
C      PRECISION FOR PLOTTING.
C
C.....OTHER SUBROUTINES NEEDED
C      ONLY BUILT-IN VERSATEC PLOTTING FUNCTIONS NEWPEN,SYMBOL &
C      NUMBER. NOTE THAT THESE ROUTINES MAY ONLY BE
C      ACCESSED WHEN RUNNING UNDER 'FORTCLGW'.
C.....
C.....SUBROUTINE CHART (N,SREY,AR,AI,SGAMMA,SLAMDA)
C
C      X0 = 2.5
C      Y0 = 6.5
C      HT = 0.15
C      HT1 = 0.7*HT
C      DELY1 = .08*HT
C      DELY2 = .065*HT1
C      DELX = .1
C
C      GRAPH TITLE
C
C      CALL NEWPEN (2)
C      CALL SYMBOL(X0,Y0,HT,'NORMALIZED PERTURBATION VELOCITY',0.,32)
C
C.....
CHAR 10
CHAR 20
CHAR 30
CHAR 40
CHAR 50
CHAR 60
CHAR 70
CHAR 80
CHAR 90
CHAR 100
CHAR 110
CHAR 120
CHAR 130
CHAR 140
CHAR 150
CHAR 160
CHAR 170
CHAR 180
CHAR 190
CHAR 200
CHAR 210
CHAR 220
CHAR 230
CHAR 240
CHAR 250
CHAR 260
CHAR 270
CHAR 280
CHAR 290
CHAR 300
CHAR 310
CHAR 320
CHAR 330
CHAR 340
CHAR 350
CHAR 360
CHAR 370
CHAR 380
CHAR 390
CHAR 400
CHAR 410
CHAR 420
CHAR 430

```



```

X0 = X0+7.*DELX
Y0 = Y0-DELY1
CALL SYMBOL(X0,Y0,HT,'FOR THE CASE N = 0',0.,18)
MESH VALUE
CALL NEWPEN(1)
X0 = X0+4.*DELX
Y0 = Y0-DELY1
SN = FLOAT(N)
CALL SYMBOL(X0,Y0,HT1,'NMESH = ',0.,9)
CALL NUMBER(999.,999.,HT1,SN,0.,-1)
REY VALUE
YC = Y0-DELY2
CALL SYMBOL(X0,Y0,HT1,'REY
CALL NUMBER(999.,999.,HT1,SREY,0.,-1)
ALPHA VALUE
X1 = X0+11.*DELY2
Y0 = Y0-DELY2
CALL SYMBOL(X0,Y0,HT1,'ALPHA = ',0.,9)
CALL NJMBER(999.,999.,HT1,AR,0.,1)
CALL NUMBER(X1,Y0,HT1,AI,0.,1)
GAMMA RL* VALUE
Y0 = Y0-DELY2
CALL SYMBOL(X0,Y0,HT1,'GAMMA* = ',0.,9)
CALL NUMBER(999.,999.,HT1,SGAMMA,0.,4)
LAMBDA VALUE
Y0 = Y0-DELY2
CALL SYMBOL(X0,Y0,HT1,'LAMBDA = ',0.,9)
CALL NUMBER(999.,999.,HT1,SLAMDA,0.,1)
SYMBOL LEGEND
Y0 = 1.75
CALL SYMBOL(X0,Y0,HT1,'OCTAGON = U(REAL)',0.,17)
Y0 = Y0-DELY2
CALL SYMBOL(X0,Y0,HT1,'DIAMOND = U(IMAG)',0.,17)
RETURN
END

```

C C C

C C C

C C C

C C C

C C C

C C C

C

CHAR 440
CHAR 450
CHAR 460
CHAR 470
CHAR 480
CHAR 490
CHAR 500
CHAR 510
CHAR 520
CHAR 530
CHAR 540
CHAR 550
CHAR 560
CHAR 570
CHAR 580
CHAR 590
CHAR 600
CHAR 610
CHAR 620
CHAR 630
CHAR 640
CHAR 650
CHAR 660
CHAR 670
CHAR 680
CHAR 690
CHAR 700
CHAR 710
CHAR 720
CHAR 730
CHAR 740
CHAR 750
CHAR 760
CHAR 770
CHAR 780
CHAR 790
CHAR 800
CHAR 810
CHAR 820
CHAR 830
CHAR 840
CHAR 850
CHAR 860
CHAR 870
CHAR 880
CHAR 890
CHAR 900

.....
THE FOLLOWING CARDS COMPRISE THE DATA DECK FOR PROGRAM EIGFCN.

/*
//GO.SYSIN DD *

DATA DECK FROM ONE RUN OF PROGRAM PIPEO (MODENO = 1)

/*
.....


```

//STB$CONT JOB ('1719,0947,AX74'),'SMC 1882',TIME=2
//EXEC FORTCLGW
//FORT.SYSIN DD *
C.....
C      PROGRAM STBCONT
C
C      PURPOSE
C
C      TO GENERATE A CONTOUR PLOT CONTAINING LINES OF INCIPIENT,
C      CRITICAL & FULLY DEVELOPED INSTABILITY USING DATA GENERATED
C      BY PROGRAM PIPEO (MODENO = 2). THE PLOT IS GENERATED ON THE
C      NPS VERSATEC PLOTTER USING SUBROUTINE PLOTG WITH ALPHA REAL
C      ON THE X-AXIS AND ALPHA IMAGINARY ON THE Y-AXIS.
C.....
C      DIMENSION X1(200), X2(200), X3(200), Y1(200), Y2(200), Y3(200)
C      COMMON /ARRAY/ G1(41,41),AR1(41),AII(41)
C      DATA X1,X2,X3,Y1,Y2,Y3/1200*0.0/
C
C      SET INITIAL VALUES
C
C      READ (5,9) NDIM
C      XMIN = -.5
C      XMAX = 0.
C      YMIN = 0.
C      YMAX = 10.
C
C      THE NEXT 3 VALUES MUST BE SET BY THE USER PRIOR TO RUNNING
C      THE PROGRAM.
C
C      SA = 47.
C      SREY = 4000.
C      SLAMDA = 0.0
C
C      READ STABILITY MAP VALUES OUTPUT BY PROGRAM PIPEO (MODENO = 2)
C
C      DO 1 I=1,NDIM
C
C      DO 1 J=1,NDIM
C      READ (5,10) AR1(I),AII(J),G1(I,J)
C      CONTINUE
C
C      COMPUTE POINTS FOR INCIPIENT,CRITICAL & FULLY DEVELOPED
C      INSTABILITY CURVES.
C
C.....

```



```

C      CALL SEARCH (-1,X1,Y1,NPLT1,NDIM)
C      CALL SEARCH (0,X2,Y2,NPLT2,NDIM)
C      CALL SEARCH (1,X3,Y3,NPLT3,NDIM)
C      JUMP TO PLOT LABEL ROUTINE IF NO INCIPIENT POINTS
C      IF (NPLT1) 8,8,2
C      IF POINTS COMPUTED, NEW PAGE AND WRITE THEM OUT
C      2 WRITE (6,11)
C      DC 3 I=1,NPLT1
C      WRITE (6,12) X1(I),Y1(I)
C      3 CONTINUE
C      PLOT INCIPIENT INSTABILITY POINTS
C      CALL PLOTG(X1,Y1,NPLT1,1,0,1,'ALPHA REAL',10,'ALPHA IMAGINARY',15,
C      $ XMIN,XMAX,YMIN,YMAX,7.,7.)
C      LEGEND FOR INCIPIENT SYMBOL
C      CALL NEWPEN (1)
C      CALL SYMBOL (1.3,0.7,.1,'OCTAGON = INCIPIENT INSTABILITY',0.,32)
C      JUMP TO PLOT LABEL ROUTINE IF NO CRITICAL POINTS
C      IF (NPLT2) 8,8,4
C      IF POINTS COMPUTED, NEW PAGE AND PRINT THEM OUT
C      4 WRITE (6,11)
C      DO 5 I=1,NPLT2
C      WRITE (6,12) X2(I),Y2(I)
C      5 CONTINUE
C      PLOT CRITICAL POINTS
C      CALL PLOTG(X2,Y2,NPLT2,2,0,2,'ALPHA REAL',10,'ALPHA IMAGINARY',15,
C      $ XMIN,XMAX,YMIN,YMAX,7.,7.)
C      LEGEND FOR CRITICAL SYMBOL

```

```

STBC 460
STBC 470
STBC 480
STBC 490
STBC 500
STBC 510
STBC 520
STBC 530
STBC 540
STBC 550
STBC 560
STBC 570
STBC 580
STBC 590
STBC 600
STBC 610
STBC 620
STBC 630
STBC 640
STBC 650
STBC 660
STBC 670
STBC 680
STBC 690
STBC 700
STBC 710
STBC 720
STBC 730
STBC 740
STBC 750
STBC 760
STBC 770
STBC 780
STBC 790
STBC 800
STBC 810
STBC 820
STBC 830
STBC 840
STBC 850
STBC 860
STBC 870
STBC 880
STBC 890
STBC 900
STBC 910
STBC 920
STBC 930

```


CALL NEWPEN (1)	STBC	940
CALL SYMBOL(1.3,.53,.1,'TRIANGLE = CRITICAL INSTABILITY',0.,31)	STBC	950
JUMP TO PLOT LABEL ROUTINE IF NO FULLY DEVELOPED POINTS	STBC	960
IF (NPLT3) 8,8,6	STBC	970
IF POINTS COMPUTED, NEW PAGE AND PRINT THEM OUT	STBC	980
6 WRITE (6,11)	STBC	990
DC 7 I=1,NPLT3	STBC	1000
WRITE (6,12) X3(1),Y3(1)	STBC	1010
7 CONTINUE	STBC	1020
PLOT FULLY DEVELOPED POINTS	STBC	1030
CALL PLOTG(X3,Y3,NPLT3,3,0,5,'ALPHA REAL',10,'ALPHA IMAGINARY',15,	STBC	1040
\$ XMIN,XMAX,YMIN,YMAX,7.,7.)	STBC	1050
LEGEND FOR FULLY DEVELOPED SYMBOL	STBC	1060
CALL NEWPEN (1)	STBC	1070
CALL SYMBOL(1.3,.36,.1,'DIAMOND = FULLY DEVELOPED INSTABILITY',	STBC	1080
\$ C.,38)	STBC	1090
LABEL THE PLOT	STBC	1100
8 CALL CHART (SN,SREY,SLAMDA)	STBC	1110
CALL PLOT (0.,0.,999)	STBC	1120
STOP	STBC	1130
9 FORMAT (I2)	STBC	1140
10 FORMAT (3E20.10)	STBC	1150
11 FORMAT ('1')	STBC	1160
12 FORMAT ('.',2E20.10)	STBC	1170
END	STBC	1180
	STBC	1190
	STBC	1200
	STBC	1210
	STBC	1220
	STBC	1230
	STBC	1240
	STBC	1250
	STBC	1260
	STBC	1270
	STBC	1280
	STBC	1290
	STBC	1300
	STBC	1310

C.....SUBROUTINE SEARCH(NCASE,X,Y,NDIM).....	SEAR	10
PURPOSE	SEAR	20
TO SCAN THE STABILITY MAP FOR CHANGES OF SIGN WITH RESPECT	SEAR	30
TO A SPECIFIED STABILITY VALUE AND GENERATE AN ARRAY OF X,Y	SEAR	40
POINTS DEFINING A CONTOUR OF THE SPECIFIED STABILITY.	SEAR	50
	SEAR	60
	SEAR	70
	SEAR	80

SEAR	90
SEAR	100
SEAR	110
SEAR	120
SEAR	130
SEAR	140
SEAR	150
SEAR	160
SEAR	170
SEAR	180
SEAR	190
SEAR	200
SEAR	210
SEAR	220
SEAR	230
SEAR	240
SEAR	250
SEAR	260
SEAR	270
SEAR	280
SEAR	290
SEAR	300
SEAR	310
SEAR	320
SEAR	330
SEAR	340
SEAR	350
SEAR	360
SEAR	370
SEAR	380
SEAR	390
SEAR	400
SEAR	410
SEAR	420
SEAR	430
SEAR	440
SEAR	450
SEAR	460
SEAR	470
SEAR	480
SEAR	490
SEAR	500
SEAR	510
SEAR	520
SEAR	530
SEAR	540
SEAR	550
SEAR	560


```

DELX = .1
GRAPH TITLE
CALL NEWPEN (2)
CALL SYMBOL(X0,Y0,HT,'STABILITY CONTOUR PLOT',0.,22)
X0 = X0+3.*DELX
YC = Y0-DELY1
CALL SYMBOL(X0,Y0,HT,'FOR THE CASE N = 0',0.,18)
MESH VALUE
CALL NEWPEN (1)
X0 = X0+4.*DELX
Y0 = Y0-DELY1
CALL SYMBOL(X0,Y0,HT1,'NMESH = ',0.,9)
CALL NUMBER (999.,999.,HT1,SN,0.,-1)
REY VALUE
Y0 = Y0-DELY2
CALL SYMBOL(X0,Y0,HT1,'REY = ',0.,9)
CALL NUMBER (999.,999.,HT1,SREY,0.,-1)
LAMBDA VALUE
YC = Y0-DELY2
CALL SYMBOL(X0,Y0,HT1,'LAMBDA = ',0.,9)
CALL NUMBER (999.,999.,HT1,SLAMDA,0.,1)
STABILITY AREA LABELS
NOTE - SINCE THE SHAPE OF THE CURVE VARIES WITH
      EACH SET OF INPUT DATA, THE COORDINATES OF THE FOLLOWING
      LABELS MUST BE ADJUSTED FOR EACH SPECIFIC PLOT.
CALL NEWPEN (2)
CALL SYMBOL(4.0,4.5,HT1,'SUPERCRITICAL',0.,13)
CALL SYMBOL(5.6,4.5,HT1,'SUBCRITICAL',0.,11)
CALL SYMBOL(6.9,4.5,HT1,'STABLE',0.,6)
YC = 4.5-DELY2
CALL SYMBOL(4.0,0,Y0,HT1,'INSTABILITY',0.,12)
CALL SYMBOL(5.6,0,Y0,HT1,'INSTABILITY',0.,11)
RETURN
END

```

```

CHAR 380
CHAR 390
CHAR 400
CHAR 410
CHAR 420
CHAR 430
CHAR 440
CHAR 450
CHAR 460
CHAR 470
CHAR 480
CHAR 490
CHAR 500
CHAR 510
CHAR 520
CHAR 530
CHAR 540
CHAR 550
CHAR 560
CHAR 570
CHAR 580
CHAR 590
CHAR 600
CHAR 610
CHAR 620
CHAR 630
CHAR 640
CHAR 650
CHAR 660
CHAR 670
CHAR 680
CHAR 690
CHAR 700
CHAR 710
CHAR 720
CHAR 730
CHAR 740
CHAR 750
CHAR 760
CHAR 770
CHAR 780
CHAR 790
CHAR 800
CHAR 810
CHAR 820
CHAR 830

```



```

.....
THE FOLLOWING CARDS CCMPRISE THE DATA DECK FOR PROGRAM STBCONT.
/*
//GD.SYSIN DD *
.
DATA DECK FROM ONE RUN OF PROGRAM PIPEO (MODENO = 2)
.
.
/*
.....

```


LIST OF REFERENCES

1. Davey, A., and Drazin, P.G., "The Stability of Poiseuille Flow in a Pipe," Journal of Fluid Mechanics, v. 36, part 2, p. 209, 22 August 1968.
2. Garg, V.K., and Rouleau, W.T., "Linear Spatial Stability of Pipe Poiseuille Flow," Journal of Fluid Mechanics, v. 54, part 1, p. 113, 6 January 1969.
3. Gill, A.E., "The Least-Damped Disturbance to Poiseuille Flow in a Circular Pipe," Journal of Fluid Mechanics, v. 61, part 1, p. 765, 3 December 1973.
4. Harrison, W.F., On the Stability of Poiseuille Flow, Ae. E. Thesis, Naval Postgraduate School, Monterey, California, 1975.
5. Huang, L.M. and Chen, T.S., "Stability of Developing Flow Subject to Non-axisymmetric Disturbances," Journal of Fluid Mechanics, v. 63, part 1, p. 183, 16 April 1973.
6. Johnston, R.H. III, A Program for the Stability Analysis of Pipe Poiseuille Flow, M.S. Thesis, Naval Postgraduate School, Monterey, California, 1976.
7. Leite, R.J., An Experimental Investigation of Axially Symmetric Poiseuille Flow, Report No. OSR-TR-56-2, Air Force Contract AF18(600)-350, November, 1956.
8. Naval Postgraduate School Report NPS-67Gn77051, Improved Finite Difference Formulas for Boundary Value Problems, by T.H. Gawain and R.E. Ball, 1 May 1977.
9. Naval Postgraduate School Report NPS67-78-006, A Basic Reformulation of the Pipe Flow Stability Problem and Some Preliminary Numerical Results, by T.H. Gawain, 1 September 1978.
10. Reynolds, O., "An Experimental Investigation of the Circumstances which Determine whether the Motion of Water Shall be Direct or Sinuous, and the Law of Resistance in Parallel Channels," Phil. Trans. Royal Soc., 174, p. 935-982, 1883.
11. Salwen, H., and Grosch, C.E., "The Stability of Poiseuille Flow in a Pipe of Circular Cross-section," Journal of Fluid Mechanics, v. 54, part 1, p. 93, 6 March 1972.

INITIAL DISTRIBUTION LIST

	No. Copies
1. Defense Documentation Center Cameron Station Alexandria, Virginia 22314	2
2. Library, Code 0142 Naval Postgraduate School Monterey, California 93940	2
3. Department Chairman, Code 67 Department of Aeronautics Naval Postgraduate School Monterey, California 93940	1
4. Prof. T.H. Gawain, Code 67Gn Department of Aeronautics Naval Postgraduate School Monterey, California 93940	5
5. LT Michael James Arnold, USN 10825 Single Tree Lane Spring Valley, California 92077	1

179850

Thesis
A7259
c.1

Arnold
Investigation of
pipe flow instability
and results for wave
number zero.

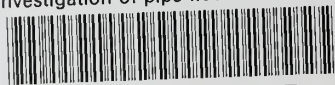
T
A
C

179850

Thesis
A7259
c.1

Arnold
Investigation of
pipe flow instability
and results for wave
number zero.

Investigation of pipe flow instability a



3 2768 002 01257 7
DUDLEY KNOX LIBRARY